Chemico-Biological Interactions 351 (2022) 109767

Contents lists available at ScienceDirect

Chemico-Biological Interactions

journal homepage: www.elsevier.com/locate/chembioint

# Ameliorating effect of continuous alpha-glycosyl isoquercitrin treatment starting from late gestation in a rat autism model induced by postnatal injection of lipopolysaccharides

Hiromu Okano [a,b], Kazumi Takashima [a,b], Yasunori Takahashi [a,b], Ryota Ojiro [a,b], Qian Tang [a,b], Shunsuke Ozawa [a,b], Bunichiro Ogawa [a], Mihoko Koyanagi [c], Robert R. Maronpot [d], Toshinori Yoshida [a,b], Makoto Shibutani [a,b,e,*]

[a] Laboratory of Veterinary Pathology, Tokyo University of Agriculture and Technology, 3-5-8 Saiwai-cho, Fuchu-shi, Tokyo, 183-8509, Japan
[b] Cooperative Division of Veterinary Sciences, Graduate School of Agriculture, Tokyo University of Agriculture and Technology, 3-5-8 Saiwai-cho, Fuchu-shi, Tokyo, 183-8509, Japan
[c] Global Scientific and Regulatory Affairs, San-Ei Gen F.F.I., Inc., 1-1-11 Sanwa-cho, Toyonaka, Osaka, 561-8588, Japan
[d] Maronpot Consulting, LLC, 1612 Medfield Road, Raleigh, NC, 27607, USA
[e] Institute of Global Innovation Research, Tokyo University of Agriculture and Technology, 3-5-8 Saiwai-cho, Fuchu-shi, Tokyo, 183-8509, Japan

ARTICLE INFO

*Keywords:*
Alpha-glycosyl isoquercitrin (AGIQ)
Autism spectrum disorder (ASD)
Hippocampal neurogenesis
Lipopolysaccharides (LPS)
Neuroinflammation
Oxidative stress

ABSTRACT

The present study investigated the role of neuroinflammation and brain oxidative stress induced by neonatal treatment with lipopolysaccharides (LPS) on the development of autism spectrum disorder (ASD)–like behaviors and disruptive hippocampal neurogenesis in rats by exploring the chemopreventive effects of alpha-glycosyl isoquercitrin (AGIQ) as an antioxidant. AGIQ was dietary administered to dams at 0.25% or 0.5% (w/w) from gestational day 18 until postnatal day (PND) 21 on weaning and then to pups until the adult stage on PND 77. The pups were intraperitoneally injected with LPS (1 mg/kg body weight) on PND 3. At PND 6, LPS alone increased Iba1$^+$ and CD68$^+$ cell numbers without changing the CD163$^+$ cell number and strongly upregulated pro-inflammatory cytokine gene expression (*Il1a*, *Il1b*, *Il6*, *Nfkb1*, and *Tnf*) in the hippocampus, and increased brain malondialdehyde levels. At PND 10, pups decreased ultrasonic vocalization (USV), suggesting the induction of pro-inflammatory responses and oxidative stress to trigger communicative deficits. By contrast, LPS alone upregulated *Nfe2l2* expression at PND 6, increased Iba1$^+$, CD68$^+$, and CD163$^+$ cell numbers, and upregulated *Tgfb1* at PND 21, suggesting anti-inflammatory responses until the weaning period. However, LPS alone disrupted hippocampal neurogenesis at weaning and suppressed social interaction parameters and rate of freezing time at fear acquisition and extinction during the adolescent stage. On PND 77, neuroinflammatory responses had mostly disappeared; however, disruptive neurogenesis and fear memory deficits were sustained. AGIQ ameliorated most changes on acute pro-inflammatory responses and oxidative stress at PND 6, and the effects on USVs at PND 10 and neurogenesis and behavioral parameters throughout the adult stage. These results suggested that neonatal LPS treatment induced acute but transient neuroinflammation, triggering the progressive disruption of hippocampal neurogenesis leading to abnormal behaviors in later life. AGIQ treatment was effective for ameliorating LPS-induced progressive changes by critically suppressing initial pro-inflammatory responses and oxidative stress.

## 1. Introduction

During the perinatal period, the immature brain passes through several essential developmental stages. During gestational and neonatal stages, the activated immune system can affect normal brain development, with long-lasting consequences on neurological and mental health [1]. Autism spectrum disorder (ASD) is a neurodevelopmental disorder

* Corresponding author. Tokyo University of Agriculture and Technology, 3-5-8 Saiwai-cho, Fuchu-shi, Tokyo, 183-8509, Japan.
*E-mail addresses:* okano-hiromu@m2.tuat.ac.jp (H. Okano), s195238q@st.go.tuat.ac.jp (K. Takashima), s194057s@st.me.tuat.ac.jp (Y. Takahashi), s204006y@st.go.tuat.ac.jp (R. Ojiro), s202349y@st.go.tuat.ac.jp (Q. Tang), s213387q@st.go.tuat.ac.jp (S. Ozawa), bunichiro_20@yahoo.co.jp (B. Ogawa), mihoko-koyanagi@saneigenffi.co.jp (M. Koyanagi), maronpot@gmail.com (R.R. Maronpot), yoshida7@cc.tuat.ac.jp (T. Yoshida), mshibuta@cc.tuat.ac.jp (M. Shibutani).

https://doi.org/10.1016/j.cbi.2021.109767
Received 16 August 2021; Received in revised form 14 November 2021; Accepted 26 November 2021
Available online 1 December 2021

**Abbreviations**

| | |
|---|---|
| AGIQ | alpha-glycosyl isoquercitrin |
| ARC | activity-regulated cytoskeleton-associated protein |
| ASD | autism spectrum disorder |
| BDNF | brain-derived neurotrophic factor |
| CA | Cornu Ammonis region |
| CALB1 | calbindin-D-28K |
| CALB2 | calbindin-D-29K |
| CD | cluster of differentiation |
| COX2 | cyclooxygenase-2 |
| DCX | doublecortin |
| FOS | Fos proto-oncogene, AP-1 transcription factor subunit |
| GABA | γ-aminobutyric acid |
| GAD67 | glutamic acid decarboxylase 67 |
| *Gapdh* | glyceraldehyde-3-phosphate dehydrogenase |
| GCL | granule cell layer |
| GD | gestational day |
| GFAP | glial fibrillary acidic protein |
| GSH | reduced glutathione |
| GSSG | glutathione disulfide |
| *Hprt1* | hypoxanthine phosphoribosyltransferase 1 |
| Iba1 | ionized calcium-binding adapter molecule 1 |
| IEG | immediate-early gene |
| IL-6 | interleukin 6 |
| KEAP1 | Kelch-like ECH-associated protein 1 |
| LPS | lipopolysaccharides |
| MDA | malondialdehyde |
| NeuN | neuronal nuclei |
| NPC | neural progenitor cell |
| NRF2 | nuclear factor erythroid 2-related factor 2 |
| NSC | neural stem cell |
| PCNA | proliferating cell nuclear antigen |
| PFA | paraformaldehyde |
| PND | postnatal day |
| PVALB | parvalbumin |
| p-ERK1/2 | phosphorylated extracellular signal-regulated kinase 1/2 |
| RELN | reelin |
| RT | reverse transcription |
| SGZ | subgranular zone |
| SOX2 | SRY-box transcription factor 2 |
| SST | somatostatin |
| TBR2 | T-box brain protein 2 |
| tGSH | total glutathione |
| TLR | Toll-like receptor |
| TNF-α | tumor necrosis factor-alpha |
| TUBB3 | tubulin, beta 3 class III |
| TUNEL | terminal deoxynucleotidyl transferase dUTP nick end labeling |
| USV | ultrasonic vocalization |

with symptoms characterized by deficits in social and communicative abilities, repetitive behaviors, or restricted areas of interest [2]. Several types of ASD have been described, such as Asperger's syndrome and pervasive developmental disorder [3], and ASD likely has multiple underlying causes. Neuroimmune alterations and inflammatory processes during brain development may contribute to the etiology of ASD [4].

Lipopolysaccharides (LPS) are a major component of gram-negative bacterial cell walls and represent a known endotoxin and potent activator of the innate immune system through interaction with the Toll-like receptor (TLR)-4. In the brain, TLR-4 is primarily expressed by microglia, astrocytes, mature neurons, and neural progenitor cells (NPCs). The hippocampus contains many cells that express TLR-4 and cytokine receptors, making the hippocampus vulnerable to the harmful effects of neuroinflammation [5]. Oxidative stress and neuroinflammation are interrelated because oxidative stress increases in inflamed tissues and can lead to cell death [6]. LPS treatment is used as an important model for the study of neuroinflammation associated with neurodegenerative diseases [7], and neonatal LPS treatment has been shown to result in changes in social behaviors and cognitive functions in rats, serving as an ASD model [8].

Adult neurogenesis has an adaptive function because newly produced neurons can integrate into and modify existing neuronal circuits [9]. The subgranular zone (SGZ) of the hippocampal dentate gyrus retains the ability to generate new neurons during adulthood. In the SGZ, type-1 neural stem cells (NSCs) undergo self-renewal and produce type-2a, type-2b, and type-3 proliferative NPCs. Type-3 NPCs differentiate to postmitotic immature granule cells, which integrate into the granule cell layer (GCL) as mature granule cells [10,11]. Neurons in the hippocampal dentate gyrus receive various projections from other brain regions, such as γ-aminobutyric acid (GABA)-ergic, cholinergic, dopaminergic, and glutamatergic inputs [12,13]. GABAergic interneurons in the hilus of the dentate gyrus have been reported to regulate granule cell differentiation and the maintenance of appropriate granule cell populations [11–13]. Both cholinergic and glutamatergic inputs to the SGZ are important for maintaining adequate levels of proliferation and differentiation among granule cell lineages [12,14]. Newly generated neurons in the hippocampus are integrated into the circuitry of existing neurons and play important roles in learning and memory; anxiety and stress regulation; and certain aspects of social behaviors [15]. Adult hippocampal neurogenesis is suppressed by LPS-induced neuroinflammation [5], and previous studies using rodent ASD models suggest that many disparate mechanisms are involved in ASD pathophysiology, including impaired neurogenesis, GABAergic imbalances, and synaptic plasticity deficits [16–18].

Alpha-glycosyl isoquercitrin (AGIQ), also known as enzymatically modified isoquercitrin, is a polyphenolic flavonol glycoside derived from the enzymatic glycosylation of rutin, which can be found in natural products, such as citrus fruits, red beans, and buckwheat [19]. AGIQ is a mixture of quercetin glycoside, consisting of isoquercitrin and its α-glucosylated derivatives, with 1–10 additional linear glucose moieties [19]. AGIQ has shown a strong radical scavenging activity, which is more pronounced than that of dibutylhydroxytoluene, a representative antioxidant, by 1,1-diphenyl-2-picrylhydrazyl method (unpublished data; San-Ei Gen F.F.I. Inc., Osaka, Japan). AGIQ presents with better water solubility and bioavailability than quercetin [20] and exerts several chemopreventive effects, including antioxidant [21], anti-inflammatory [21], antihypertensive [22], anti-allergic [20], and tumor-suppressive [23] effects. In addition, AGIQ can pass the blood-brain barrier and is distributed in the brain [24]. While there are no available studies reporting transplacental or translactational transfer of AGIQ to offspring, ameliorating effects on disease conditions have been revealed in offspring by developmental exposure to quercetin or isoquercitrin [25,26]. Recently, we also reported the facilitation of fear extinction learning in a contextual fear conditioning test following continuous AGIQ exposure starting during the developmental stages in rats [27,28]. Furthermore, developmental hypothyroidism-induced disruptive neurogenesis was ameliorated due to the restoration of antioxidant system and neurogenesis-regulatory system involving GABAergic interneuron subpopulations after postweaning continuous AGIQ exposure [29].

The present study was conducted to investigate the role of neuroinflammation and brain oxidative stress on the development of disruptive brain functions induced by neonatal LPS treatment in rats. For this purpose, we examined the chemopreventive effects of AGIQ as an

antioxidant and anti-inflammatory agent against LPS-induced ASD-like behaviors and disruptive hippocampal neurogenesis. AGIQ was continuously administered to dams starting during the late gestation and lactation periods, and AGIQ administration continued in pups after weaning and throughout the adult stage. The time-dependent effects of neonatal LPS treatment and the chemopreventive effect of AGIQ were examined with respect to neuroinflammation, oxidative stress, communicative and learning abilities, and hippocampal neurogenesis.

## 2. Materials and methods

### 2.1. Chemicals and animals

LPS from *Escherichia coli* O55:B5 purified by phenol extraction (EC No. 297-473-0; purity: 97%) was purchased from Sigma-Aldrich Co. LLC. (St. Louis, MO, USA). AGIQ (purity: > 97%) was provided by San-Ei Gen F.F.I. Inc.. Mated female Slc:SD rats were purchased from Japan SLC, Inc. (Hamamatsu, Japan) at gestational day (GD) 1 (appearance of vaginal plug was designated as GD 0). Pregnant rats were individually housed in polycarbonate cages with paper bedding until day 21 after delivery. Animals were maintained in an air-conditioned animal room (temperature: 23 ± 2°C, relative humidity: 55 ± 15%) with a 12-h light/dark cycle. Pregnant rats were allowed free access to a powdered basal diet (CRF-1; Oriental Yeast Co. Ltd., Tokyo, Japan) until the start of exposure to AGIQ and access to tap water ad libitum throughout the experimental period. From postnatal day (PND) 21 (where PND 0 is the day of delivery) onwards, pups were reared with three or four animals per cage and provided powdered basal diet with or without AGIQ and tap water ad libitum.

### 2.2. Experimental design

#### 2.2.1. Main study

The main study was conducted to examine behaviors in terms of open field test, social interaction test, and contextual fear conditioning test during the adolescent and adult stages, brain oxidative stress, neuroinflammatory responses, and hippocampal neurogenesis in infancy and at weaning and adult stage (Fig. 1). Pregnant rats were randomly assigned to four groups (controls, LPS alone, LPS + 0.25% AGIQ, and LPS + 0.5% AGIQ) of 15 animals per group before starting AGIQ treatment at GD 18. AGIQ mixed with 0.25% or 0.5% (w/w) in the powdered basal diet was administered to dams from GD 18 to post-delivery day 21 and to pups from PND 21 to PND 77. The high dose of AGIQ in the present study has been shown to facilitate fear extinction learning by continuous exposure from the gestational stages to adulthood [27,28]. In the main study, body weight, and food and water consumption of dams were measured every 3–5 days throughout the experimental period. Because neurogenesis is influenced by circulating levels of steroid hormones during the estrous cycle [30], male pups were selected for all analyses in the main study. On PND 2, the litters were randomly culled to preserve 5–8 male pups and 0–3 female pups per litter (total of 8 pups per litter). On PND 3, male pups were administrated LPS at 1 mg/kg body weight intraperitoneally or saline to controls. The dosage, route and timing of LPS treatment were determined based on the results of the previous study showing induction of robust microglia activation, aberrant hippocampal neurogenesis, and deficits in communicative and cognitive functions [8]. The pups were weighed every 3–4 days until PND 21 and measured body weight, food and water consumption once a week until PND 77. On PND 6, 10 male pups per group (one pup per dam) were euthanized by exsanguination from the abdominal aorta under deep anesthetization with $CO_2/O_2$, and removed

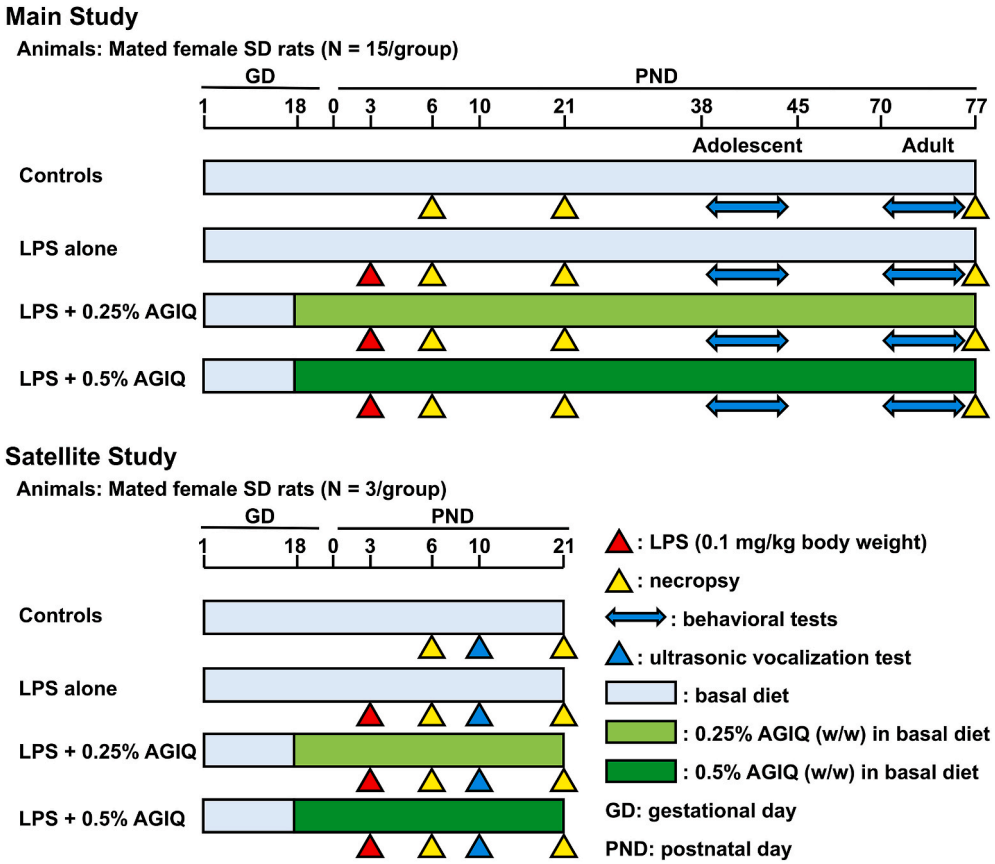


**Fig. 1.** Experimental design of developmental exposure study of lipopolysaccharides (LPS) and alpha-glycosyl isoquercitrin (AGIQ) using mated female SD rats. Animal experiments consist of main study and satellite study.

brains were fixed in methacarn solution for 5 h at room temperature and then immersed in 100% ethanol for immunohistochemical analysis. On PND 21, 10–12 male pups per group (one pup per dam) were subjected to perfusion fixation for immunohistochemical analysis through the left cardiac ventricle with ice-cold 4% (w/v) paraformaldehyde (PFA) in 0.1 M phosphate buffer (pH 7.4) at a flow rate of 10 mL/min after deep anesthetization with $CO_2/O_2$. For mRNA expression analysis on PND 21, 6–12 male pups (one pup per dam) were euthanized by exsanguination from the abdominal aorta under $CO_2/O_2$ anesthesia and their brains were removed, weighed and fixed according to the whole brain fixation method using methacarn solution [31]. For measurement of oxidative stress levels in the brain on PND 21, 7–13 male pups per group (one pup per dam) were subjected to blood perfusion through the left cardiac ventricle with ice-cold saline [0.9% (w/v) sodium chloride] at a flow rate of 10 mL/min and removed the brain after deep anesthetization with $CO_2/O_2$. The hippocampal tissues were excised from the cerebral hemisphere on ice, immediately frozen in liquid nitrogen and stored at −80 °C until analysis. Ten male pups per group were examined for behavioral tests during each of the adolescent stage (PND 38–45) and adult stage (PND 70–77). Different animals were used for behavioral tests between the adolescent and adult stages. On PND 77, 10 male pups per group that have not been examined in behavioral tests during the adult stage were subjected to perfusion fixation with ice-cold 4% PFA buffer solution at a flow rate of 35 mL/min after deep anesthetization with $CO_2/O_2$ for immunohistochemical analysis of neurogenesis-related and glial cell marker proteins. In addition, all animals subjected to behavioral tests (open field test, social interaction test and contextual fear conditioning test) during the adult stage were similarly subjected to perfusion fixation for immunohistochemical analysis of synaptic plasticity-related proteins. For mRNA expression analysis on PND 77, 6–10 male pups per group were euthanized for brain sampling in a similar fashion with PND 21.

#### 2.2.2. Satellite study

Satellite study was conducted to examine brain oxidative stress and neuroinflammatory responses, as well as ultrasonic vocalization (USV) during early postnatal life (Fig. 1). The group composition and treatment protocol of LPS and AGIQ were the same as those in the main study, and 3 mated female rats per group were used. On PND 2, the litters were randomly culled to preserve 4–6 male pups and 4–6 female pups per litter (total of 10 pups per litter). Because estrous cycle of rat does not resume during lactation period in dam [32] and does not begin in infancy [33], either male or female pups were selected for each analysis in the satellite study. On PND 6, 7 male pups per group were euthanized by exsanguination from the abdominal aorta under $CO_2/O_2$ anesthesia and their brains were removed for measurement of oxidative stress levels. Cerebral hemisphere samples were excised and immediately frozen in liquid nitrogen and stored at −80 °C until analysis. For mRNA expression analysis on PND 6 in terms of oxidative stress and neuroinflammatory responses, 7 male pups per group were similarly euthanized and removed brains were subjected to whole-brain fixation using methacarn solution as aforementioned. On PND 10, 6–10 female pups per group were examined for USV test.

In both of main and satellite studies, all dams and remaining female pups were euthanized at PND 21 by exsanguination from the abdominal aorta under $CO_2/O_2$ anesthesia.

All animal experiments in the present study were conducted in accordance with the National Institutes of Health guide for the care and use of laboratory animals (NIH Publications No. 8023, revised 1978), and all efforts were made to minimize animal suffering. The experimental procedures were approved by the Animal Care and Use Committee of the Tokyo University of Agriculture and Technology (approved No.: 31–38 for main study; 31–64 for satellite study).

### 2.3. Behavioral tests

USV test was performed using lactating pups, and open field test, social interaction test, and contextual fear conditioning test were performed using adolescent and adult animals. All behavioral tests were conducted in the behavior room adjacent to the animal room. In each behavioral test, the apparatus was cleaned with 70% ethanol solution every time when each animal was tested. After the cessation of each test, each animal was promptly returned to the home cage and transferred to the animal room. All experiments were conducted during the period between 08:00 and 19:00, and the order of animal selection for test among groups was balanced to avoid any bias (e.g., by circadian hormonal fluctuations) in each group.

#### 2.3.1. USV test

The USV test was performed on PND 10 using female pups in the satellite study to assess the parameters related to mother-child communication. The test took place in polycarbonate observation cages (172 mm width × 240 mm depth × 129 mm height) that were placed in a sound-attenuating chamber (CL-4211; O'Hara & Co., Ltd., Tokyo, Japan) maintained at 50 lux luminance and 50 dB white noise. In order to collect USVs of test animals, a microphone with an integrated preamplifier (4158 HN; O'Hara & Co., Ltd.) was placed in the center of the observation cage with the sound-collecting tip directly above the animals so that the animals could not touch it. The test animal was transferred from the home cage to the observation cage and the 5–95 kHz USV was recorded for 5 min per animal using interface (USV-1010AF; O'Hara & Co., Ltd.) and recoding software (URS-9100; O'Hara & Co., Ltd.). Because 40 kHz USV is emitted by pups during social isolation when separated from mother and littermates in rats [34], 38–42 kHz USV of tested animals were extracted by ultrasonic wave analysis software (UWA-9100; O'Hara & Co., Ltd.) and subjected to calculation of USV parameters (call counts, and average and maximum durations per call). USV test was conducted during 13:00–19:00.

#### 2.3.2. Open field test

Open field test was performed on PND 38 (adolescent stage) and PND 70 (adult stage) using male pups in the main study to assess the parameter related to locomotor activity and anxiety-like behaviors and to habituate to the arena that will be used in the social interaction test on the following days (Supplementary Fig. 1). The arena consisted of a square stainless-steel tray with black polyvinyl plastic surface and walls with a black polyvinyl plastic surface surrounding the tray (900 mm width × 900 mm depth × 500 mm height; O'Hara & Co., Ltd.). The floor illuminance was 20 lux in the center of the arena. Animals were transferred from the animal room to the behavior test room 1–1.5 h before the start of the experiment and habituated to the behavior test room. The test animal was placed at the corner of the arena with the head facing the wall and allowed to explore the arena freely for 10 min. The total moving distance and time spent in the center or wall area of the field were recorded by a CCD camera (WAT-902B; Watec Co., Ltd., Tsuruoka, Japan) mounted above the arena and evaluated by an automatic video-tracking system (TimeOFCR1 software; O'Hara & Co., Ltd.). In the video-tracking analysis, the field was equally divided into 25 square areas, and the central 9 areas were defined as the center region, and the percentage of time spent in the center region or wall side was calculated.

#### 2.3.3. Social interaction test

Social interaction test was performed on PND 39 and PND 40 (adolescent stage) and on PND 71 and PND 72 (adult stage) using male pups in the main study to assess the ability to recognize novel animal and the sociality to novel animal (Supplementary Fig. 1). The test consisted of session 1 (PND 39 and PND 71) and session 2 (PND 40 and PND 72). The floor illuminance was 20 lux in the center of the arena. Animals were transferred from the animal room to the behavior test room 1–1.5 h before the start of the experiment and habituated to the behavior test

room. In session 1 (habituation to the mesh cage), the mesh cage (SI-MBR, 200 mm width × 150 mm depth × 300 mm height; O'Hara & Co., Ltd.) without the novel animal was set up at the corner of the same arena as used in the open field test. The test animal was placed on the opposite side of the mesh cage with the head facing the wall and allowed to explore the arena freely for 5 min. The moving distance and exploration time toward the mesh cage were recorded by a CCD camera (WAT-902B; Watec Co., Ltd.) mounted above the arena and evaluated by an automatic video-tracking system (TimeSSI software; O'Hara & Co., Ltd.). In the video-tracking analysis, the area around the mesh cage was divided into "Contact area radius", "In radius", and "Out radius" and social interaction parameters (moving distance around the mesh cage, contact counts into contact area radius, and spent time around mesh cage) were calculated. In session 2, unfamiliar animals were placed in the mesh cage and the test animal was examined for 3 min. The same analysis as in session 1 was conducted. Among the animals in the control group, the unfamiliar animals were selected as those from different home cages than the animals used for behavioral tests. Four animals of average body weight were selected and used for each test in turn.

#### 2.3.4. Contextual fear conditioning test

Contextual fear conditioning test was conducted during the periods from PND 41 to PND 45 (adolescent stage) and from PND 73 to PND 77 (adult stage) using male pups in the main study. Five trials in the order of "fear conditioning", "fear acquisition", and "fear extinction trial #1, #2, and #3" were performed with 24 h interval during 5 consecutive days (Supplementary Fig. 1). The test took place in a rodent observation cage (30 × 37 × 25 cm) constructed of Plexiglas that was placed in a sound-attenuating chamber (CL-4211; O'Hara & Co., Ltd.). The chamber was kept at 50 dB white noise, and at 50 lux luminance. The floor of the chamber consisted of 21 steel rods through which a scrambled shock from a shock generator (SGA-2020; O'Hara & Co., Ltd.) was delivered. Animals were transferred from the animal room to the behavior test room 1–1.5 h before the start of the experiment and habituated to the behavior test room. In the trial of contextual fear conditioning, animals were transferred from the home cage to the observation cage and after 88, 148, and 238 s, they received 2 s footshocks (0.3 mA intensity, a total of 3 footshocks). Animals were removed from the observation cage 60 s after the final footshock and returned to the home cages. Thus, it took 5 min for the trial. In the trial of contextual fear acquisition and extinction, animals were placed back into the original training context for 5 min, but during which no footshock was delivered. Animals examined during the adult stage were euthanized 90 min after the 3rd fear extinction session for immunohistochemical analysis of synaptic plasticity-related proteins in the GCL to examine their maximal induction in response to behavioral stimuli [28]. Animals' behavior was video recorded by a CCD camera (WAT-902B; O'Hara & Co., Ltd.) and analyzed the rate of freezing time using an automatic video tracking system (TimeFZ2 software; O'Hara & Co., Ltd.). The rate of freezing time was defined as the percent of time the rat spent in freezing behavior for ≥2 s during each of the trial time of 5 min.

### 2.4. Measurement of oxidative stress parameters in the brain

Lipid peroxidation levels were analyzed by measuring the accumulation of thiobarbituric acid-reactive substances in the brain tissue and expressed as malondialdehyde (MDA) content using Lipid Peroxidation (MDA) Assay Kit (Abcam plc, Cambridge, UK). The brain tissue samples (N = 7 per group, cerebral tissues at PND 6 and hippocampal tissues at PND 21) were homogenized in a lysis buffer solution containing dibutyl hydroxytoluene. The homogenates were reacted with thiobarbituric acid at 95°C for 60 min. Then, the MDA-thiobarbituric acid adducts were extracted with n-butanol and their concentrations were determined spectrophotometrically at 532 nm using a microplate reader. The protein concentration of each tissue homogenate was determined using a Bicinchoninic Acid Protein Assay Kit (Thermo Fisher Scientific, Waltham, MA, USA) to quantitate concentration of MDA (nmol/mg tissue protein).

Glutathione disulfide (GSSG) and reduced glutathione (GSH) levels in the brain tissue were measured on both PND 6 and PND 21 using GSSG/GSH Quantification Kit (Dojindo Laboratories, Kumamoto, Japan). The brain tissue samples (N = 7 per group, cerebral tissues at PND 6 and hippocampal tissues at PND 21) were homogenized in a 5% 5-sulfosalicylic acid solution. Diluted supernatants were assayed for GSSG/GSH levels according to the manufacturer's protocol. The absorbance of the samples was determined spectrophotometrically at 405 nm using a microplate reader. Total glutathione (tGSH: GSH plus GSSG) and GSSG concentrations (μmol/L) were calculated using standard curves for tGSH and GSSG. The GSH concentration (μmol/L) was calculated from these two concentrations. The ratio of GSSG to GSH concentrations was then determined.

### 2.5. Immunohistochemistry and apoptosis assay

#### 2.5.1. Immunoreactive and apoptotic cell detection in the hippocampal dentate gyrus

Three mm-thick coronal slices were prepared at −2.2 mm from the bregma of the perfusion-fixed brains at PND 21 and PND 77 using a brain matrix. In the case of methacarn-fixed brains at PND 6, 4 mm-thick coronal slices were made at the position of the optic chiasm to include hippocampal formation. Brain slices were further fixed with 4% PFA buffer solution (PND 21 and PND 77) or 100% ethanol (PND 6) overnight at 4 °C, routinely embedded in paraffin and sectioned at 3 μm.

Brain sections were subjected to immunohistochemical analysis using primary antibodies against the following (Supplementary Table 1): glial fibrillary acidic protein (GFAP), which is expressed in type-1 NSCs (radial glial cells) in the SGZ and astrocytes [35]; SRY-box transcription factor 2 (SOX2), which is expressed in type-1 NSCs and type-2a NPCs in the SGZ [35]; T-box brain protein 2 (TBR2), expressed in type-2b NPCs in the SGZ [35]; doublecortin (DCX), which is expressed in type-2b and type-3 NPCs and immature granule cells in the SGZ and GCL [35]; tubulin, beta 3 class III (TUBB3, also known as Tuj-1), which is expressed mainly in postmitotic immature granule cells in the SGZ and GCL [36]; neuronal nuclei (NeuN), which is expressed in postmitotic neurons of both immature and mature granule cells in the SGZ and GCL [35]; and calbindin-D-28K (CALB1), calbindin-D-29K (CALB2), glutamic acid decarboxylase 67 (GAD67), parvalbumin (PVALB), reelin (RELN), and somatostatin (SST), which are expressed in GABAergic interneurons [12,37]; ionized calcium-binding adapter molecule 1 (Iba1), a microglia-specific molecule in the brain [38]; cluster of differentiation (CD) 68, a general microglia/macrophage marker [39]; CD163, a M2 microglia/macrophage marker [39]; proliferating cell nuclear antigen (PCNA), a cell proliferation marker; Fos proto-oncogene, AP-1 transcription factor subunit (FOS), activity-regulated cytoskeleton-associated protein (ARC), and cyclooxygenase-2 (COX2), which are members of the immediate-early gene (IEG) proteins involved in synaptic plasticity [40]; phosphorylated extracellular signal-regulated kinase 1/2 (p-ERK1/2; phosphorylated p44/p42 MAP kinase), a member of the mitogen activated protein kinase family that is activated by phosphorylation to promote transcriptional programs leading to the induction of *Arc* and *Fos* [41,42].

Avidin-Biotin Complex method was used in immunohistochemical staining and hematoxylin was used for counter staining. Deparaffinized sections were incubated in 0.3% hydrogen peroxide solution in absolute methanol for 30 min to quench the endogenous peroxidase. Conditions of antigen retrieval applied for some primary antibodies were shown in Supplementary Table 1. The sections and primary antibody were reacted overnight at 4 °C. Immunodetection was performed using a Vectastain® Elite ABC kit (Vector Laboratories, Burlingame, CA, USA) with 3,3′-diaminobenzidine/$H_2O_2$ as the chromogen. One section per animal was subjected to each immunohistochemical analysis.

For detection of apoptosis in the SGZ and GCL, a terminal

deoxynucleotidyl transferase dUTP nick end labeling (TUNEL) assay was carried out using an *In situ* Apoptosis Detection kit (Takara Bio Inc., Kusatsu, Japan), with 3,3′-diaminobenzidine/$H_2O_2$ as the chromogen. One section per animal was subjected to TUNEL assay.

#### 2.5.2. Quantification of immunoreactive and apoptotic cell in the hippocampal dentate gyrus

In the brain samples of PND 21 and PND 77, $GFAP^+$, $SOX2^+$ or $TBR2^+$ cells of granule cell lineages, $PCNA^+$ proliferating cells in the SGZ of the dentate gyrus were bilaterally counted and normalized for the length of the SGZ (Supplementary Fig. 2). $DCX^+$, $TUBB3^+$ or $NeuN^+$ cells of granule cell lineages distributed in the SGZ and GCL, and $ARC^+$, $COX2^+$, $FOS^+$ or p-$ERK1/2^+$ granule cells in the GCL were bilaterally counted and normalized for the length of SGZ. $TUNEL^+$ apoptotic cells counted in both of the SGZ and GCL respectively and normalized for the length of the SGZ. GABAergic interneuron subpopulations distributed within the hilus of the dentate gyrus, i.e., $CALB1^+$, $CALB2^+$, $GAD67^+$, $PVALB^+$, $RELN^+$ or $SST^+$ cells, were bilaterally counted and normalized per area unit of the hilar area (polymorphic layer). Glial cell populations distributed within the dentate gyrus hilus, i.e., $Iba1^+$, $CD68^+$, $CD163^+$ or $GFAP^+$ cells were also similarly counted and normalized per area unit. In the brain samples of PND 6, glial cell populations, i.e., $Iba1^+$, $CD68^+$, $CD163^+$ or $GFAP^+$ cells, were bilaterally counted and normalized per area unit of the whole area of hippocampal formation (Supplementary Fig. 2). The number of each immunoreactive cell population except for $NeuN^+$ cells was manually counted while blinded to the treatment conditions under microscopic observation using a BX51 microscope (Olympus Corporation, Tokyo, Japan). In the case of $NeuN^+$ cell counting, digital photomicrographs at × 100-fold magnification were taken using a BX51 microscope attached to a DP26 Digital Camera System (Olympus Corporation), and the immunoreactive cells were counted automatically applying the WinROOF image analysis software package (version 5.7; Mitani Corporation, Fukui, Japan). Immunoreactive neurons located inside of the Cornu Ammonis region (CA) 3, consisting of large pyramidal neurons were excluded from the counting in the hilus of the dentate gyrus. The length of the SGZ and the area of the hilus were measured by applying the cellSens image analysis software package (standard package 1.9; Olympus Corporation).

### 2.6. Transcript-level expression analysis in the hippocampal dentate gyrus

The mRNA expression in the hippocampal dentate gyrus of male pups were examined at PND 6, PND 21 and PND 77 using real-time reverse transcription (RT)-PCR. Two-mm-thick coronal brain slices were prepared at −3.0 mm from the bregma of methacarn-fixed brains on PND 21 and PND 77 using a brain matrix, then dentate gyrus tissue was collected from the slice using a biopsy punch with a 1-mm pore size (Kai Industries Co. Ltd. Gifu, Japan). In case of the brains at PND 6, 2 mm-thick coronal slices were made at the position of the optic chiasm, then dentate gyrus tissue was collected from the slice. Total RNA from the tissue sample was extracted using RNeasy Mini Kit (Qiagen, Hilden, Germany) according to the manufacturer's protocol. First-strand cDNA was synthesized using SuperScript® III Reverse Transcriptase (Thermo Fisher Scientific) from 1 μg total RNA. The target genes for real-time RT-PCR and the sequence of the primers for each gene are shown in Supplementary Table 2. The primer sequences of genes for real-time RT-PCR, except for *Il6*, were designed using Primer Express software (Version 3.0; Thermo Fisher Scientific) or Primer-BLAST (NCBI, https://www.ncbi.nlm.nih.gov/tools/primer-blast/). The primer sequences of *Il6* were identical to those used in previous reports [43]. Real-time PCR with Power SYBR® Green PCR Master Mix (Thermo Fisher Scientific) was performed using a StepOnePlus™ Real-time PCR System (Thermo Fisher Scientific). The relative transcript level of target genes in each group to the controls was determined by the $2^{-\Delta\Delta C}{}_T$ method [44], using hypoxanthine phosphoribosyltransferase 1 (*Hprt1*) and glyceraldehyde-3-phosphate dehydrogenase (*Gapdh*) gene as the endogenous controls in the same sample.

### 2.7. Statistical analysis

Numerical data were presented as mean ± SD. Significant differences between the controls and LPS alone were evaluated as follows. Levene's test was applied for homogeneity of variance. When the variance was homogenous between the groups, Student's *t*-test was applied, and in case of heterogeneous data, Aspin-Welch's *t*-test was performed. Significant differences between the LPS alone and LPS +0.25% AGIQ or LPS +0.5% AGIQ group were evaluated as follows. Levene's test was applied for homogeneity of variance. If the variance was homogenous, numerical data were assessed using Dunnett's test. In case of heterogeneous data, Aspin Welch's *t*-test with Bonferroni correction was applied. All analyses were performed using IBM SPSS Statistics ver. 25 (IBM Corporation, Armonk, NY, USA), and $P < 0.05$ was considered statistically significant.

## 3. Results

### 3.1. In life parameter data and necropsy data

After LPS treatment at PND 3, 20–30% of male pups died within a few days (Supplementary Table 3). Body weight of male pups in the LPS alone significantly decreased from PND 6 to PND 40 compared with controls but the food and water consumption were not statistically different compared with the controls (Supplementary Table 4). Body weight of male pups in the LPS +0.5% AGIQ group significantly decreased from PND 3 to PND 13 and from PND 23 to PND 77 compared with the LPS alone. Food consumption of male pups in the LPS +0.25% AGIQ group significantly decreased at PND 23, and that in the LPS +0.5% AGIQ group significantly decreased at PND 23 and PND 34, compared with the LPS alone. Water consumption of male pups in the LPS +0.5% AGIQ group significantly decreased at PND 23, PND 34, and PND 48 compared with the LPS alone.

At necropsies on PND 6 and PND 21, body weight in the LPS alone significantly decreased compared with the controls (Supplementary Table 5). On PND 21, brain weight in the LPS alone significantly decreased compared with the controls. On PND 77 necropsy, body and brain weights were unchanged between the controls and LPS alone and between the LPS alone and any of the LPS + AGIQ groups.

### 3.2. Behavioral test

#### 3.2.1. USV test

Total call counts, maximum duration per call, and average duration per call were significantly decreased in the LPS alone compared with the controls. Total call counts and average duration per call in the LPS +0.5% AGIQ group and maximum duration per call in the LPS +0.25% AGIQ group were significantly increased compared with the LPS alone (Fig. 2, Supplementary Table 6).

#### 3.2.2. Open field test

Open field test conducted during both adolescent and adult stages, any parameters related to locomotor and anxiety were not statistically different between the controls and LPS alone and between the LPS alone and any of the LPS + AGIQ groups (Supplementary Table 7).

#### 3.2.3. Social interaction test

During the adolescent stage, any parameters examined were not statistically different between the controls and LPS alone and between the LPS alone and any of the LPS + AGIQ groups when using empty mesh cage only (Supplementary Table 8). In contrast, when novel animal was added to the mesh cage, moving distance around the mesh cage was significantly decreased in the LPS alone compared with the controls. This value was significantly increased in the LPS +0.5% AGIQ group

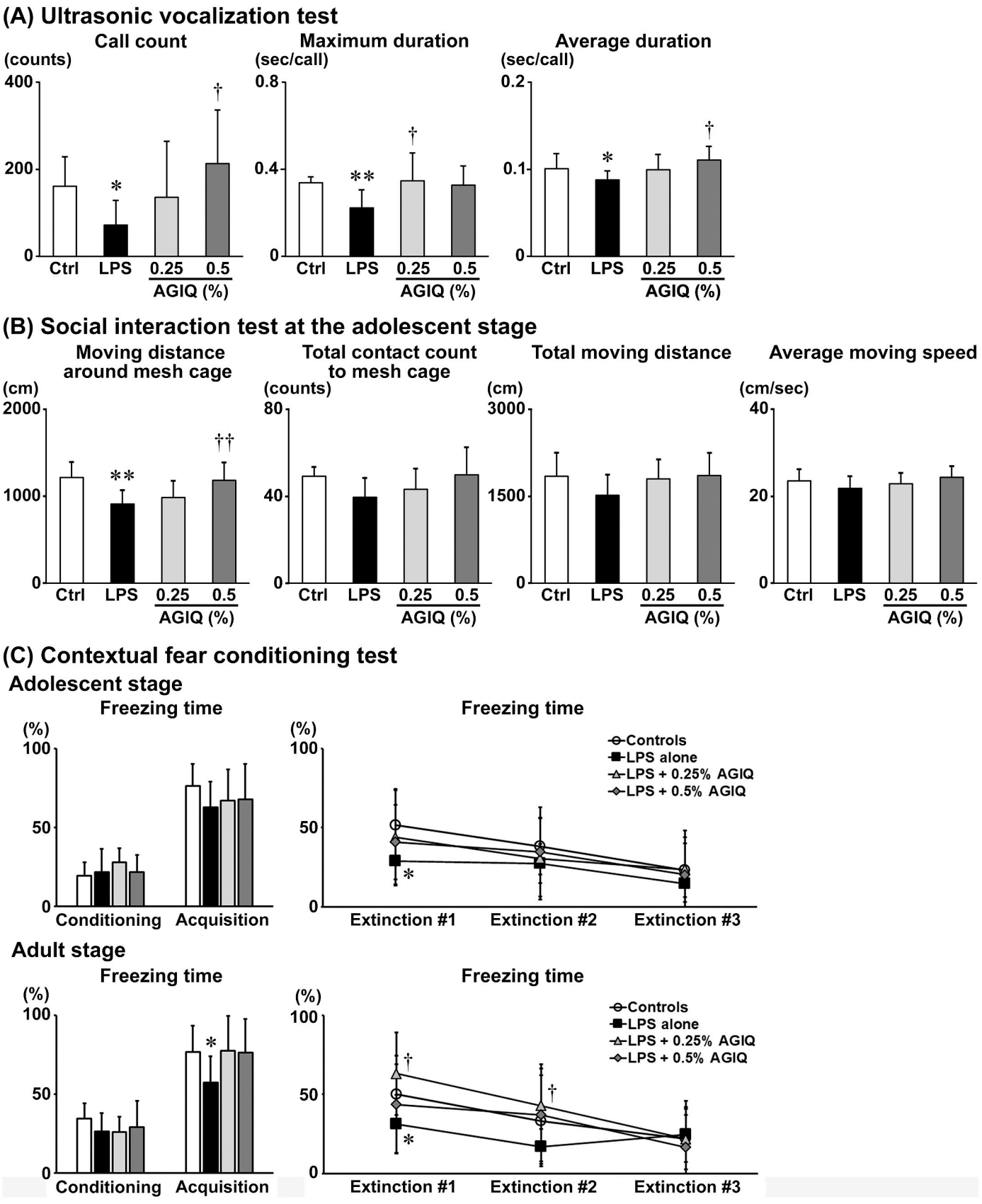


**Fig. 2.** The results of behavioral tests. (A) Ultrasonic vocalization test in female pups at postnatal day (PND) 10. N = 6 (controls) or 10 (other groups). (B) Social interaction test in male pups during the adolescent stage (session 2; PND 39–40). N = 10/group. (C) Contextual fear conditioning test in male pups during the adolescent stage (PND 41–45) and adult stage (PND 73–77). N = 10/group. Values are expressed as the mean +SD or mean ± SD. $^{*}P < 0.05$, $^{**}P < 0.01$, significantly different from the controls by Student's *t*-test or Aspin–Welch's *t*-test. $^{\dagger}P < 0.05$, $^{\dagger\dagger}P < 0.01$, significantly different from the LPS alone by Dunnett's test or Aspin–Welch's *t*-test with Bonferroni correction.

compared with the LPS alone (Fig. 2, Supplementary Table 8).

During the adult stage, any parameters were not statistically different between the controls and LPS alone and between the LPS alone and any of the LPS + AGIQ groups (Supplementary Table 9).

#### 3.2.4. Contextual fear conditioning test

During the adolescent stage, the rate of freezing time at all trials except for the 1st trial of fear extinction were not statistically different between the controls and LPS alone and between the LPS alone and any of the LPS + AGIQ groups (Fig. 2, Supplementary Table 10). The rate of freezing time of the 1st trial of fear extinction in the LPS alone was significantly decreased compared with the controls.

During the adult stage, the rate of freezing time of the fear conditioning trial was not statistically different between the controls and LPS alone and between the LPS alone and any of the LPS + AGIQ groups (Fig. 2, Supplementary Table 10). The rate of freezing time of the fear acquisition trial in the LPS alone was significantly decreased compared with the controls. The rate of freezing time of the fear extinction trial in LPS alone was significantly decreased compared with the controls at the 1st trial and this value of the LPS +0.25% AGIQ group was significantly increased compared with the LPS alone at the 1st and 2nd trials.

### 3.3. Immunohistochemical analysis

#### 3.3.1. Numbers of glial cell populations in the hippocampal formation

On PND 6, number of Iba1$^+$ microglia/macrophages was significantly increased in the LPS alone compared with the controls and this value was significantly decreased in both of the LPS + AGIQ groups compared with the LPS alone (Fig. 3, Supplementary Table 11). Number of CD68$^+$ microglia/macrophages was significantly increased in the LPS alone compared with the controls; however, AGIQ treatment did not significantly alter the number compared with the LPS alone. Number of CD163$^+$ microglia/macrophages was not significantly different between the controls and LPS alone and between the LPS alone and any of the LPS + AGIQ groups. Number of GFAP$^+$ astrocytes was significantly increased in the LPS alone compared with the controls and was significantly decreased in both of the LPS + AGIQ groups compared with the LPS alone.

On PND 21, number of Iba1$^+$ microglia/macrophages was significantly increased in the LPS alone compared with the controls and was significantly decreased in the LPS +0.25% AGIQ group compared with the LPS alone (Fig. 3, Supplementary Table 12). Number of CD68$^+$ microglia/macrophages was significantly increased in the LPS alone

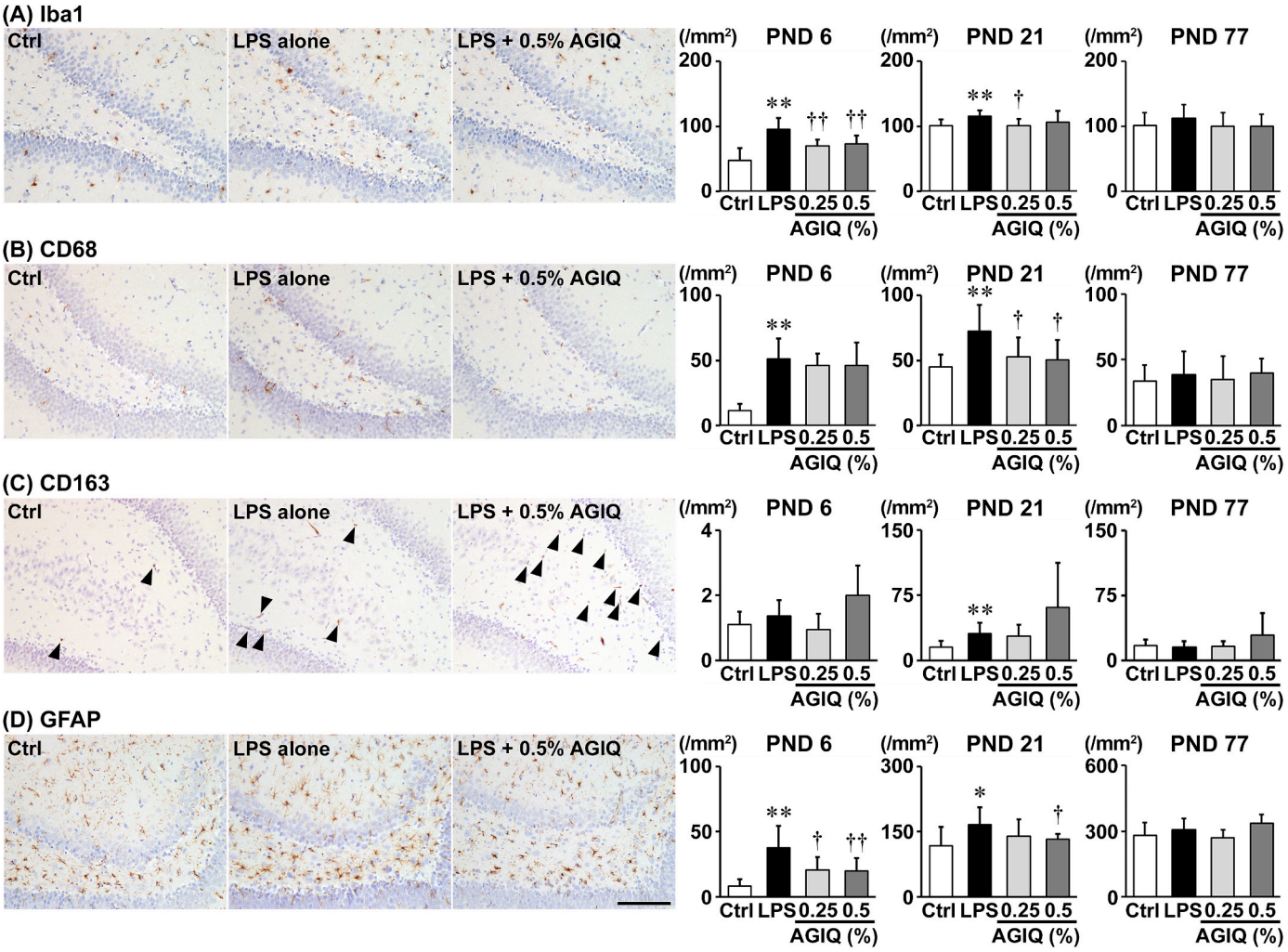


**Fig. 3.** Distribution of immunoreactive cells for glial cell marker proteins, i.e., (A) ionized calcium-binding adapter molecule 1 (Iba1), (B) cluster of differentiation (CD) 68, (C) CD163, and (D) glial fibrillary acidic protein (GFAP) in the hippocampal formation at postnatal day (PND) 6 and hilar region of the dentate gyrus at PND 21 and PND 77 of male pups. Representative images from the controls (left), LPS alone (middle), and LPS + 0.5% AGIQ (right) on PND 21. Arrowheads indicate immunoreactive cells. Magnification × 200; bar = 100 μm. Graphs show the numbers of immunoreactive cells in the hippocampal formation at PND 6 and hilar region at PND 21 and PND 77. N = 10/group. Values are expressed as the mean +SD. *$P < 0.05$, **$P < 0.01$, significantly different from the controls by Student's *t*-test or Aspin–Welch's *t*-test. $^{\dagger}P < 0.05$, $^{\dagger\dagger}P < 0.01$, significantly different from the LPS alone by Dunnett's test or Aspin–Welch's *t*-test with Bonferroni correction.

compared with the controls and was significantly decreased in both of the LPS + AGIQ groups compared with the LPS alone. Number of CD163$^+$ microglia/macrophages was significantly increased in the LPS alone compared with the controls; however, AGIQ treatment did not significantly alter the number compared with the LPS alone. Number of GFAP$^+$ astrocytes was significantly increased in the LPS alone compared with the controls and was significantly decreased in the LPS +0.5% AGIQ group compared with the LPS alone.

On PND 77, numbers of Iba1$^+$, CD68, or CD163$^+$ microglia/macrophages and GFAP$^+$ astrocytes were not significantly different between the controls and LPS alone and between the LPS alone and any of the LPS + AGIQ groups (Fig. 3, Supplementary Table 13).

### 3.3.2. Numbers of granule cell lineage subpopulations in the SGZ and/or GCL

On PND 21, number of NeuN$^+$ cells was significantly decreased in the LPS alone compared with the controls and was significantly increased in the LPS +0.5% AGIQ group compared with the LPS alone (Fig. 4, Supplementary Table 12). With regard to the numbers of GFAP$^+$, SOX2$^+$, TBR2$^+$, DCX$^+$, and TUBB3$^+$ cells, there were no significant differences between the controls and LPS alone and between the LPS alone and any of the LPS + AGIQ groups.

On PND 77, numbers of DCX$^+$ and TUBB3$^+$ cells were significantly decreased in the LPS alone compared with the controls and number of TUBB3$^+$ cells was significantly increased in the LPS +0.5% AGIQ group compared with the LPS alone (Fig. 4, Supplementary Table 13). With regard to the numbers of GFAP$^+$, SOX2$^+$, TBR2$^+$, and NeuN$^+$ cells, there were no significant differences between the controls and LPS alone and between the LPS alone and any of the LPS + AGIQ groups.

### 3.3.3. Cell proliferation activity and apoptotic cell numbers in the SGZ and/or GCL

On PND 21, number of PCNA$^+$ proliferating cells showed no significant difference between the controls and LPS alone and between the LPS alone and any of the LPS + AGIQ groups (Fig. 5, Supplementary Table 12). Number of TUNEL$^+$ apoptotic cells in the SGZ was significantly increased in the LPS alone compared with the controls; however, AGIQ treatment did not significantly alter the number compared with the LPS alone. Number of TUNEL$^+$ cells in the GCL showed no significant difference between the controls and LPS alone and between the LPS alone and any of the LPS + AGIQ groups.

On PND 77, number of PCNA$^+$ proliferating cells was significantly increased in the LPS alone compared with the controls; however, AGIQ treatment did not significantly alter the number compared with the LPS alone (Fig. 5, Supplementary Table 13). Number of TUNEL$^+$ apoptotic cells distributed in the SGZ and GCL showed no significant difference between the controls and LPS alone and between the LPS alone and any of the LPS + AGIQ groups.

### 3.3.4. Numbers of interneuron subpopulations in the hilus of the dentate gyrus

On PND 21, numbers of GAD67$^+$ and PVALB$^+$ interneurons were significantly decreased in the LPS alone compared with the controls; however, AGIQ treatment did not significantly alter the number compared with the LPS alone (Fig. 6, Supplementary Table 12). There were no significant differences in the numbers of CALB1$^+$, CALB2$^+$, RELN$^+$, and SST$^+$ interneurons between the controls and LPS alone and between the LPS alone and any of the LPS + AGIQ groups.

On PND 77, number of GAD67$^+$ interneurons was significantly increased in the LPS alone compared with the controls; however, AGIQ treatment did not significantly alter the number compared with the LPS alone (Fig. 6, Supplementary Table 13). There were no significant differences in the numbers of CALB1$^+$, CALB2$^+$, PVALB$^+$, RELN$^+$ and SST$^+$ interneurons between the controls and LPS alone and between the LPS alone and any of the LPS + AGIQ groups.

### 3.3.5. Numbers of immunoreactive cells for synaptic plasticity-related proteins in the GCL

On PND 21, numbers of FOS$^+$ or p-ERK1/2$^+$ cells showed no significant difference between the controls and the LPS alone but were significantly increased in the LPS +0.5% AGIQ group compared with the LPS alone (Fig. 7, Supplementary Table 12). Numbers of ARC$^+$ and COX2$^+$ cells showed no significant differences between the controls and LPS alone and between the LPS alone and any of the LPS + AGIQ groups.

On PND 77, numbers of ARC$^+$ and FOS$^+$ cells were significantly increased in the LPS alone compared with the controls; however, AGIQ treatment did not significantly alter the number compared with the LPS alone (Fig. 7, Supplementary Table 13). Number of COX2$^+$ or p-ERK1/2$^+$ cells showed no significant difference between the controls and LPS alone and between the LPS alone and any of the LPS + AGIQ groups.

## 3.4. Transcript-level expression changes in the hippocampus

### 3.4.1. Inflammation and oxidative stress-related genes in the hippocampal formation or dentate gyrus

On PND 6, transcript levels of *Il1a*, *Il1b*, *Il6*, *Nfkb1*, *Tgfb1,* and *Tnf* among genes encoding chemical mediators and related molecules were significantly increased in the hippocampal formation of the LPS alone after normalization with *Gapdh* and/or *Hprt1* compared with the controls (Table 1). Transcript levels of *Il1a* and *Il1b* were significantly decreased in both of the LPS + AGIQ groups after normalization with *Gapdh* and *Hprt1* compared with the LPS alone. Transcript levels of *Keap1* and *Nfe2l2* among oxidative stress-related genes were significantly increased in the hippocampal formation of the LPS alone after normalization with *Gapdh* and/or *Hprt1* compared with the controls. On the other hand, transcript level of *Nfe2l2* was significantly decreased in the LPS + 0.5% AGIQ group after normalization with *Gapdh* compared with the LPS alone.

On PND 21 and PND 77, transcript level of *Il1a* among genes encoding chemical mediators and related molecules was significantly increased in the dentate gyrus of the LPS alone after normalization with *Gapdh* and *Hprt1* compared with the controls; however, AGIQ treatment did not alter the transcript level compared with the LPS alone (Table 1). Transcript levels of any oxidative stress-related genes in the dentate gyrus examined on PND 21 showed no significant difference between the controls and LPS alone and between the LPS alone and any of the LPS + AGIQ groups.

### 3.4.2. Neurogenesis-related genes in the dentate gyrus

On PND 21, transcript level of *Rbfox3* (also known as NeuN) among granule cell lineage marker genes was significantly decreased in the LPS alone after normalization with *Gapdh* and *Hprt1* compared with the controls and was significantly increased in both of the LPS + AGIQ groups after normalization with *Gapdh* and *Hprt1* compared with the LPS alone (Table 2). Transcript level of *Pvalb* among GABAergic interneuron marker genes was significantly decreased in the LPS alone after normalization with *Hprt1* compared with the controls, and transcript level of *Calb1* was significantly increased in the LPS +0.5% AGIQ group after normalization with *Gapdh* compared with the LPS alone. Transcript level of *Chrna7* among cholinergic receptor genes was significantly increased in the LPS +0.5% AGIQ group after normalization with *Hprt1* compared with the LPS alone. Transcript level of *Drd2*, a dopaminergic receptor gene, was significantly decreased in the LPS +0.5% AGIQ group after normalization with *Gapdh* and *Hprt1* compared with the LPS alone. Transcript level of *Gria2* among genes encoding glutamatergic receptors and glutamate transporters were significantly decreased in the LPS alone after normalization with *Gapdh* compared with the controls. Transcript level of *Ptgs2* among synaptic plasticity-related genes was significantly decreased in the LPS alone after normalization with *Hprt1* compared with the controls and was significantly increased in both of the LPS + AGIQ groups after normalization with *Gapdh* and *Hprt1* compared with the LPS alone. Transcript level of *Bdnf* among neurotrophic factor-

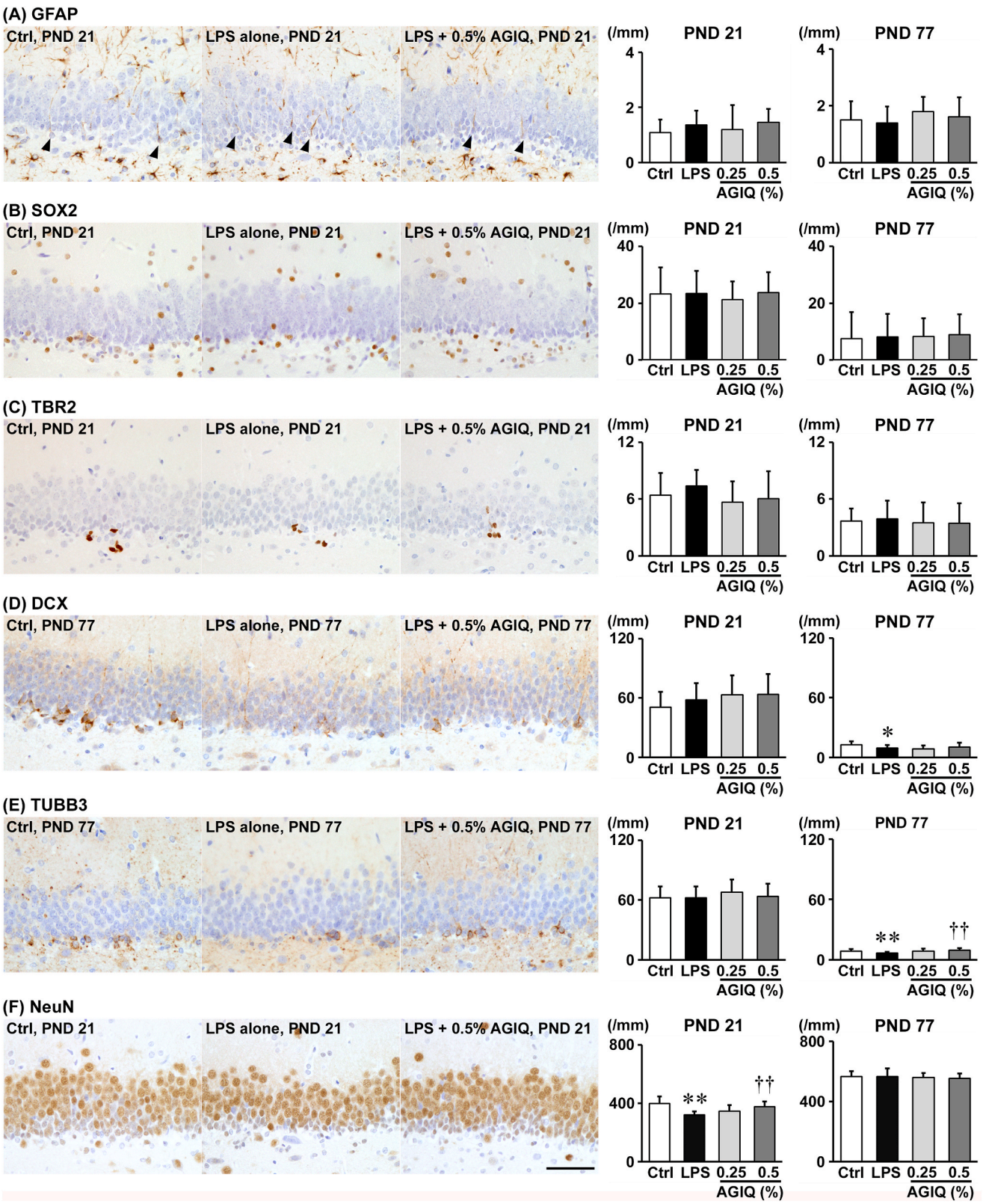


**Fig. 4.** Distribution of immunoreactive cells for granule cell lineage marker proteins, i.e., (A) glial fibrillary acidic protein (GFAP), (B) SRY-box transcription factor 2 (SOX2), or (C) T-box brain protein 2 (TBR2) in the subgranular zone (SGZ), and (D) doublecortin (DCX), (E) tubulin, beta 3 class III (TUBB3), or (F) neuronal nuclei (NeuN) in the SGZ and granule cell layer (GCL) of male pups at postnatal day (PND) 21 and PND 77. Representative images from the controls (left), LPS alone (middle), and LPS + 0.5% AGIQ (right) at PND 21 (GFAP, SOX2, TBR2 and NeuN) or PND 77 (DCX and TUBB3). Arrowheads indicate immunoreactive cells. Magnification × 400; bar = 50 μm. Graphs show the numbers of immunoreactive cells in the SGZ and/or GCL. N = 10/group. Values are expressed as the mean +SD. *$P < 0.05$, **$P < 0.01$, significantly different from the controls by Student's *t*-test or Aspin–Welch's *t*-test. $^{\dagger\dagger}P < 0.01$, significantly different from the LPS alone by Dunnett's test or Aspin–Welch's *t*-test with Bonferroni correction.

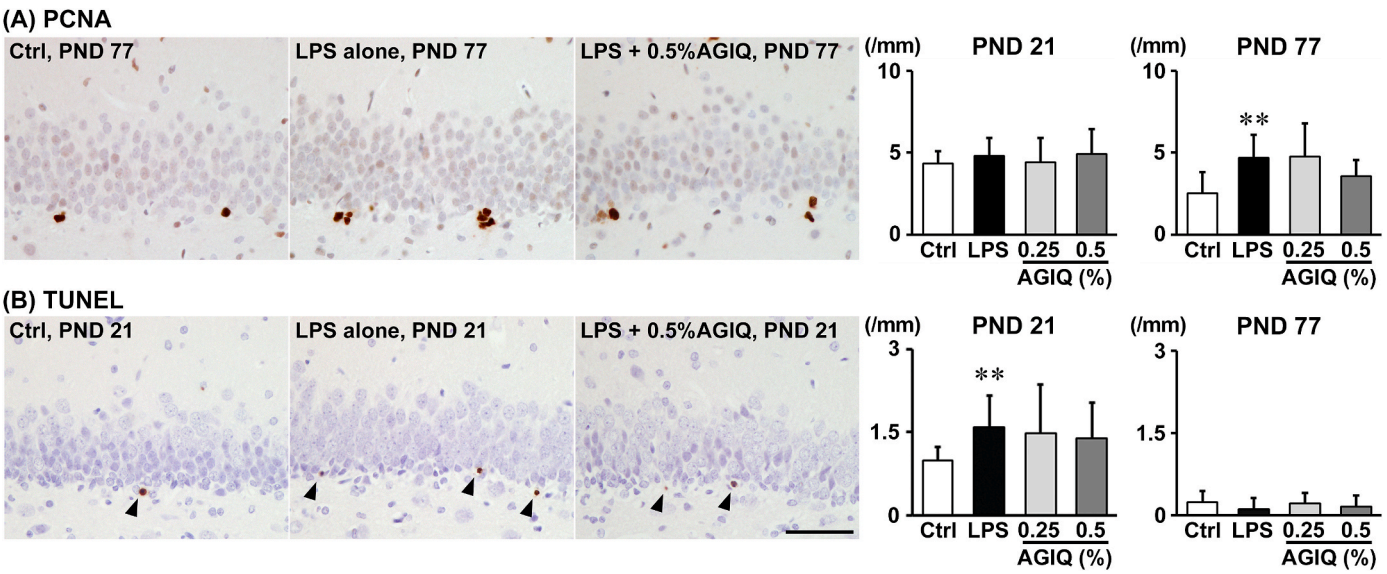


**Fig. 5.** Distribution of (A) proliferating cell nuclear antigen (PCNA)$^+$ proliferating cells and (B) terminal deoxynucleotidyl transferase dUTP nick end labeling (TUNEL)$^+$ apoptotic cells in the subgranular zone (SGZ) of male pups at postnatal day (PND) 21 and PND 77. Representative images from the controls (left), LPS alone (middle) and LPS + 0.5% AGIQ (right) at PND 21 (TUNEL) or PND 77 (PCNA). Arrowheads indicate immunoreactive cells. Magnification × 400; bar = 50 μm. Graphs show the numbers of immunoreactive cells in the SGZ. N = 10/group. Values are expressed as the mean +SD. $^{**}P < 0.01$, significantly different from the controls by Student's *t*-test or Aspin–Welch's *t*-test.

related genes was significantly increased in the LPS +0.5% AGIQ group after normalization with *Gapdh* and *Hprt1* compared with the LPS alone.

On PND 77, transcript level of *Tubb3* among granule cell lineage marker genes in the LPS alone was significantly decreased after normalization with *Gapdh* and *Hprt1* compared with the controls and the level in both of the LPS + AGIQ groups was significantly increased after normalization with *Gapdh* and/or *Hprt1* compared with the LPS alone (Table 3). Transcript level of *Chrna7* among cholinergic receptor genes was significantly decreased in the LPS + 0.25% AGIQ group after normalization with *Gapdh* compared with the LPS alone. Transcript levels of *Gria1*, *Gria2* and *Gria3* among genes encoding glutamatergic receptors were significantly decreased in either or both of the LPS + AGIQ groups after normalization with *Gapdh* compared with the LPS alone. Transcript level of *Arc* among synaptic plasticity-related genes was significantly increased in the LPS alone after normalization with *Gapdh* and *Hprt1* compared with the controls and was significantly decreased in both of the LPS + AGIQ groups after normalization with *Gapdh* and *Hprt1* compared with the LPS alone. Transcript level of *Cntf* among neurotrophic factor-related genes was significantly increased in the LPS alone after normalization with *Gapdh* compared with the controls, and transcript level of *Ntrk2* was significantly decreased in the LPS +0.25% AGIQ group after normalization with *Gapdh* compared with the LPS alone.

### 3.5. Oxidative stress level in the brain

On PND 6, MDA level in the cerebrum was significantly increased in the LPS alone compared with the controls (Fig. 8, Supplementary Table 14). On PND 21, MDA level in the hippocampus was significantly decreased in the LPS +0.25% AGIQ group compared with the LPS alone. GSSG/GSH ratio was not statistically different between the controls and LPS alone and between the LPS alone and any of the LPS + AGIQ groups on both PND 6 and PND 21.

## 4. Discussion

In the present study, LPS alone increased Iba1$^+$ microglia/macrophages and GFAP$^+$ astrocytes and upregulated the transcript levels of inflammatory cytokines, such as *Il1a*, *Il1b*, *Il6,* and *Tnf,* on PND 6. The number of CD68$^+$ cells also increased following LPS treatment, whereas the numbers of CD163$^+$ cells were very low in all groups at this time point. CD68 is expressed in the activated isoforms of both M1-type pro-inflammatory and M2-type anti-inflammatory microglia/macrophages [45], and CD163 is expressed in M2 microglia/macrophages [39]. Because interleukin 6 (IL-6) and tumor necrosis factor-alpha (TNF-α) are M1 markers that cause pro-inflammatory neurodestructive responses [46,47], these results suggest that LPS activates M1-polarized microglia/macrophages shortly after neonatal exposure. In this study, LPS alone upregulated *Tgfb1* expression on PND 6, which encodes transforming growth factor β, a potent inflammatory suppressor [48]. *Tgfb1* upregulation may, therefore, reflect the induction of anti-inflammatory responses starting only a few days after LPS treatment. The simultaneous increase in the GFAP$^+$ astrocyte population may also reflect a neuroprotective response because astrocytes play roles in the innate and adaptive immune responses against neural tissue injury [49]. In this study, AGIQ treatment decreased the populations of Iba1$^+$ microglia/macrophages and GFAP $^+$ astrocytes and downregulated or showed a trend for downregulation of *Il1a*, *Il1b*, and *Tnf* compared with the LPS alone on PND 6, whereas CD68$^+$ cell numbers remained unchanged. These results suggested a neuroprotective function for AGIQ against LPS-induced acute neuroinflammation.

On PND 21, LPS alone increased both CD68$^+$ and CD163$^+$ cell numbers, in addition to Iba1$^+$ cell numbers, and non-significantly upregulated *Tgfb1*. These results suggested the induction of an anti-inflammatory response mediated by the transition from the M1 phenotype at PND 6 to the M2 phenotype at weaning. A sustained increase in GFAP$^+$ astrocytes suggested an anti-inflammatory response. By contrast, AGIQ decreased the CD68$^+$ population at both doses and retained or increased the numbers of CD163$^+$ cells compared with the LPS alone. AGIQ caused the further upregulation of *Tgfb1* at both doses, which suggested that AGIQ may enhance anti-inflammatory responses. AGIQ decreased or showed a decreasing trend in the numbers of GFAP$^+$ astrocytes compared with the LPS alone, suggesting the amelioration of initial pro-inflammatory responses. On PND 77, all LPS-induced glial cell population changes and changes in the expression of chemical mediator genes disappeared in AGIQ-treated animals, except for the continued upregulation of *Il1a*, suggesting the amelioration of neuroinflammation during the adult stage.

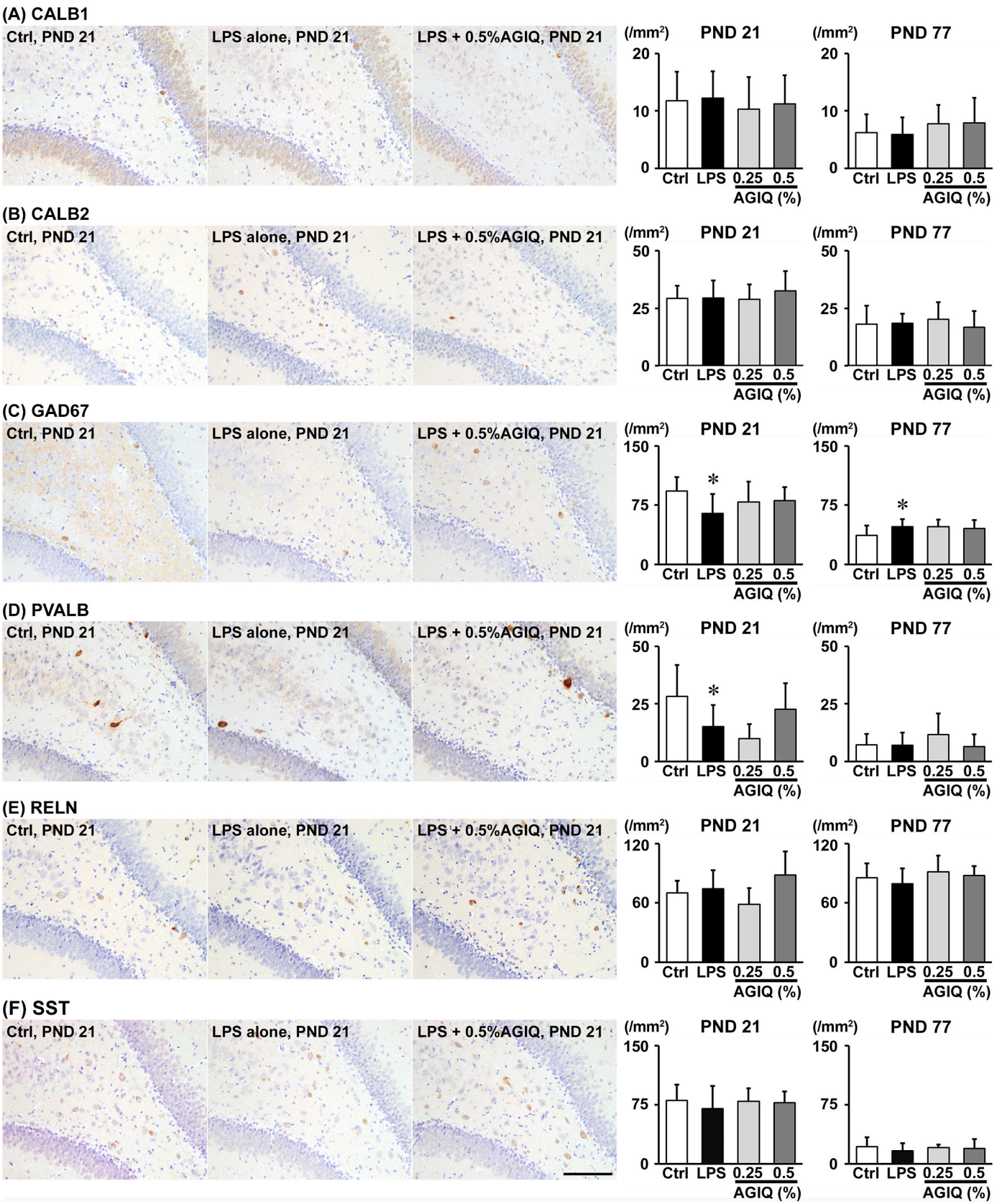


**Fig. 6.** Distribution of interneurons immunoreactive for (A) calbindin-D-28K (CALB1), (B) calbindin-D-29K (CALB2), (C) glutamic acid decarboxylase 67 (GAD67), (D) parvalbumin (PVALB), (E) reelin (RELN), and (F) somatostatin (SST) in the hilar region of the dentate gyrus of male pups at postnatal day (PND) 21 and PND 77. Representative images from the controls (left), LPS alone (middle), and LPS + 0.5% AGIQ (right) at PND 21. Magnification × 200; bar = 100 μm. Graphs show the numbers of immunoreactive cells in the hilar region. N = 10/group. Values are expressed as the mean +SD. *$P < 0.05$, significantly different from the controls by Student's *t*-test or Aspin–Welch's *t*-test.

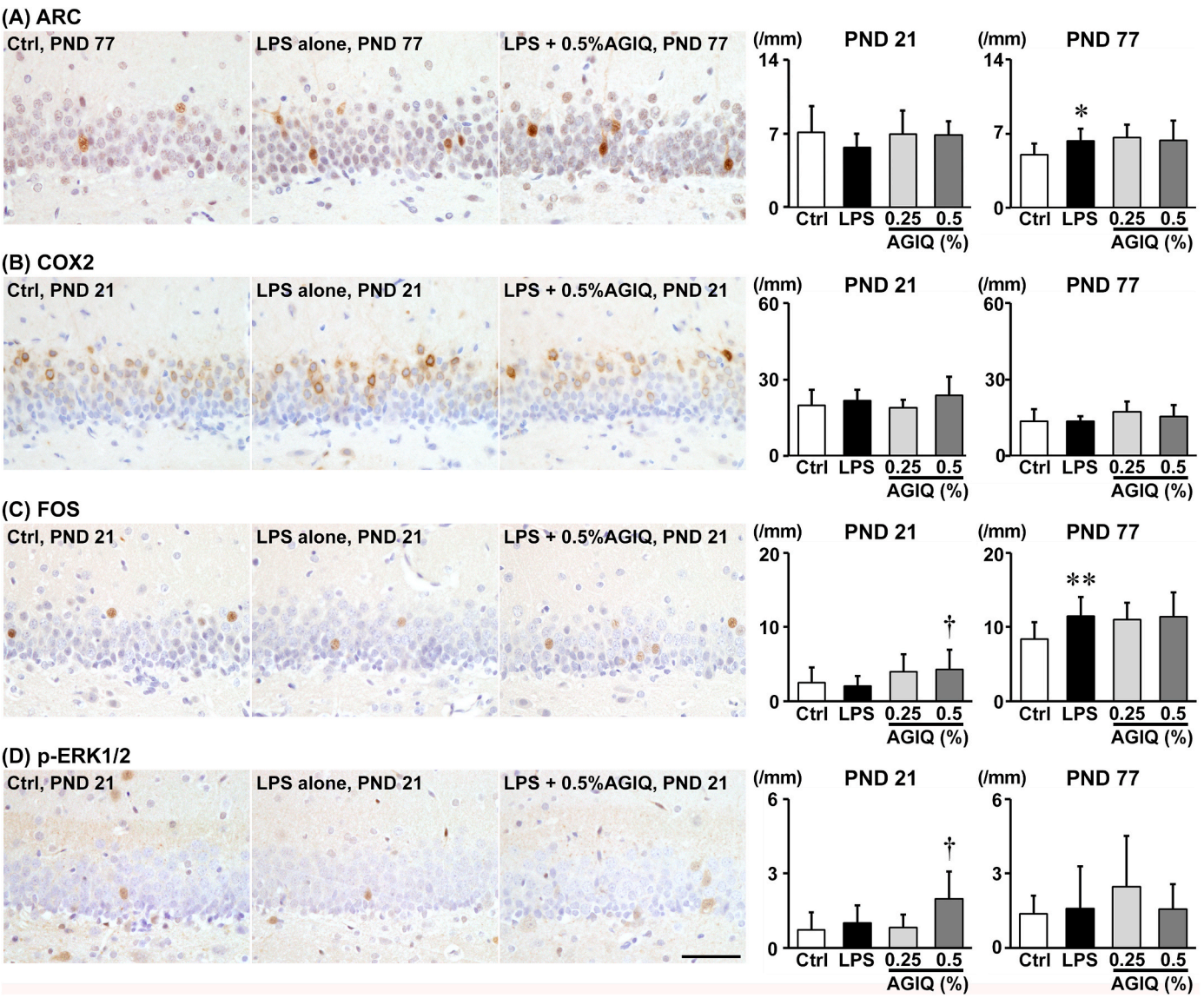


**Fig. 7.** Distribution of granule cells immunoreactive for synaptic plasticity-related proteins, i.e., (A) activity-regulated cytoskeleton-associated protein (ARC), (B) cyclooxygenase-2 (COX2), (C) Fos proto-oncogene, AP-1 transcription factor subunit (FOS), and (D) phosphorylated extracellular signal-regulated kinase 1/2 (p-ERK1/2) in the granule cell layer (GCL) of male pups at postnatal day (PND) 21 and PND 77. PND 77 animals were those examined at 90 min after the 3rd trial of fear extinction test. Representative images from the controls (left), LPS alone (middle), and LPS + 0.5% AGIQ (right) at PND 21 (COX2, FOS, and p-ERK1/2) or PND 77 (ARC). Magnification × 400; bar = 50 μm. Graphs show the numbers of immunoreactive cells in the GCL. N = 10/group. Values are expressed as the mean +SD. $^{*}P < 0.05$, $^{**}P < 0.01$, significantly different from the controls by Student's *t*-test or Aspin–Welch's *t*-test. $^{\dagger}P < 0.05$, significantly different from the LPS alone by Dunnett's test or Aspin–Welch's *t*-test with Bonferroni correction.

Intracerebral LPS injection has previously been shown to increase MDA levels and the GSSG/GSH ratio, which are both major oxidative stress markers in the rat brain [50]. In the present study, LPS alone increased cerebral MDA levels and the cerebral GSSG/GSH ratio compared with the controls at PND 6, although the latter change was non-significant. These results suggested that oxidative brain damage was induced shortly after systemic LPS treatment. Although the observed values were non-significantly different from those observed for LPS alone, AGIQ restored cerebral MDA levels and the GSSG/GSH ratio at PND 6, suggesting an antioxidant effect that provides neuroprotection against LPS-induced brain damage. LPS alone also upregulated *Keap1* and *Nfe2l2* in the hippocampal formation on PND 6. *Keap1* encodes Kelch-like ECH-associated protein 1 (KEAP1), which acts as a cysteine thiol–rich sensor of redox insults, whereas *Nfe2l2* encodes nuclear factor erythroid 2-related factor 2 (NRF2), which is a transcription factor that robustly transduces chemical signals to regulate a battery of cytoprotective genes [51]. KEAP1 represses NRF2 activity under quiescent conditions; however, NRF2 is liberated from KEAP1-mediated repression upon exposure to various stresses [51], and NRF2 activation skews macrophage polarization toward an M2 phenotype, exerting anti-inflammatory effects [52]. Therefore, the activation of the KEAP1–NRF2 system shortly after neonatal LPS treatment suggests the activation of a cellular defense against oxidative stress, moving toward an anti-inflammatory phenotype, which is observed at weaning. The MDA level and the GSSG/GSH ratio reverted to control levels at weaning, even after neonatal LPS treatment.

In the present study, LPS alone decreased $NeuN^{+}$ cells in the SGZ and GCL, representing both immature and mature granule cells [11], and downregulated the expression of *Rbfox3*, which encodes NeuN, in the dentate gyrus at PND 21. These animals did not present altered numbers of $TUBB3^{+}$ cells, which represent immature granule cells [36], and the transcript levels of *Tubb3* and *Dpysl3*, which are marker genes of

**Table 1**
Transcript-level expression changes of inflammation and oxidative stress-related genes in the hippocampal formation or dentate gyrus in male pups.

| | Control | | LPS alone | | LPS + 0.25% AGIQ | | LPS + 0.5% AGIQ | |
|---|---|---|---|---|---|---|---|---|
| | Relative transcript level normalized to | | | | | | | |
| | *Gapdh* | *Hprt1* | *Gapdh* | *Hprt1* | *Gapdh* | *Hprt1* | *Gapdh* | *Hprt1* |
| **PND 6** | | | | | | | | |
| **Chemical mediators and related markers** | | | | | | | | |
| *Il1a* | 1.32 ± 1.04 | 1.17 ± 0.73 | 13.43 ± 3.99[b] | 10.29 ± 1.65[b] | 5.06 ± 1.67[d] | 4.21 ± 1.52[d] | 7.03 ± 2.18[d] | 6.11 ± 2.48[d] |
| *Il1b* | 1.46 ± 1.47 | 1.34 ± 1.21 | 40.30 ± 19.04[b] | 33.86 ± 12.96[b] | 11.64 ± 5.95[d] | 10.34 ± 4.41[d] | 14.05 ± 8.24[d] | 14.12 ± 9.69[d] |
| *Il4* | 1.02 ± 0.21 | 1.02 ± 0.24 | 1.36 ± 0.36 | 1.23 ± 0.31 | 1.21 ± 0.38 | 1.03 ± 0.25 | 1.12 ± 0.13 | 0.97 ± 0.21 |
| *Il6* | 1.25 ± 0.96 | 1.22 ± 0.74 | 3.33 ± 1.66[a] | 2.56 ± 1.35 | 2.30 ± 1.56 | 1.87 ± 1.27 | 2.51 ± 1.57 | 2.43 ± 1.85 |
| *Nfkb1* | 1.11 ± 0.51 | 1.07 ± 0.34 | 2.28 ± 0.87[a] | 1.73 ± 0.37 | 1.57 ± 0.25 | 1.30 ± 0.21 | 1.55 ± 0.32 | 1.32 ± 0.39 |
| *Tgfb1* | 1.09 ± 0.42 | 1.13 ± 0.54 | 1.92 ± 0.62[b] | 1.48 ± 0.35 | 1.81 ± 0.76 | 1.54 ± 0.67 | 1.70 ± 0.30 | 1.45 ± 0.39 |
| *Tnf* | 1.05 ± 0.35 | 1.06 ± 0.40 | 2.46 ± 1.15[a] | 1.86 ± 0.61[a] | 1.56 ± 0.48 | 1.28 ± 0.36 | 1.48 ± 0.37 | 1.28 ± 0.47 |
| **Oxidative stress-related markers** | | | | | | | | |
| *Cat* | 1.17 ± 0.68 | 1.26 ± 0.93 | 1.58 ± 1.01 | 1.29 ± 0.93 | 1.33 ± 0.49 | 1.10 ± 0.44 | 1.10 ± 0.69 | 0.95 ± 0.61 |
| *Gpx1* | 1.09 ± 0.53 | 1.06 ± 0.37 | 2.98 ± 3.01 | 2.49 ± 2.59 | 2.01 ± 0.99 | 1.71 ± 0.89 | 1.59 ± 1.38 | 1.30 ± 1.01 |
| *Hmox1* | 1.11 ± 0.45 | 1.12 ± 0.43 | 1.22 ± 0.09 | 1.03 ± 0.15 | 1.60 ± 0.36 | 1.31 ± 0.23 | 1.39 ± 0.19 | 1.20 ± 0.38 |
| *Keap1* | 1.15 ± 0.52 | 1.15 ± 0.45 | 2.04 ± 0.74[a] | 1.56 ± 0.36 | 1.46 ± 0.29 | 1.20 ± 0.17 | 1.50 ± 0.27 | 1.29 ± 0.42 |
| *Nfe2l2* | 1.13 ± 0.52 | 1.13 ± 0.46 | 2.68 ± 1.25[a] | 2.03 ± 0.67[a] | 1.65 ± 0.42 | 1.36 ± 0.37 | 1.56 ± 0.36[c] | 1.37 ± 0.59 |
| *Mt1* | 1.06 ± 0.37 | 1.06 ± 0.33 | 2.00 ± 1.08 | 1.50 ± 0.52 | 1.93 ± 0.59 | 1.57 ± 0.38 | 1.84 ± 0.46 | 1.63 ± 0.75 |
| *Sod1* | 1.02 ± 0.23 | 1.02 ± 0.21 | 1.33 ± 0.32 | 1.09 ± 0.38 | 1.10 ± 0.16 | 0.92 ± 0.19 | 1.03 ± 0.24 | 0.87 ± 0.27 |
| **PND 21** | | | | | | | | |
| **Chemical mediators and related markers** | | | | | | | | |
| *Il1a* | 1.19 ± 0.69 | 1.21 ± 0.69 | 2.67 ± 0.77[b] | 2.61 ± 1.05[a] | 1.74 ± 0.45 | 1.79 ± 0.55 | 2.53 ± 1.82 | 2.19 ± 1.26 |
| *Il1b* | 1.12 ± 0.51 | 1.13 ± 0.58 | 2.31 ± 1.24 | 2.20 ± 1.25 | 2.08 ± 1.33 | 2.08 ± 1.18 | 2.38 ± 2.35 | 1.97 ± 1.61 |
| *Il4* | 1.01 ± 0.19 | 1.02 ± 0.23 | 1.03 ± 0.16 | 0.96 ± 0.16 | 1.04 ± 0.23 | 1.11 ± 0.31 | 0.95 ± 0.12 | 1.01 ± 0.17 |
| *Il6* | 1.01 ± 0.18 | 1.01 ± 0.14 | 1.04 ± 0.40 | 1.01 ± 0.46 | 0.91 ± 0.17 | 0.94 ± 0.26 | 1.00 ± 0.21 | 0.95 ± 0.40 |
| *Nfkb1* | 1.00 ± 0.05 | 1.00 ± 0.09 | 1.02 ± 0.22 | 0.99 ± 0.30 | 0.92 ± 0.10 | 0.96 ± 0.25 | 1.18 ± 0.51 | 1.08 ± 0.48 |
| *Tgfb1* | 1.37 ± 1.10 | 1.30 ± 0.97 | 1.38 ± 0.67 | 1.38 ± 0.82 | 1.71 ± 1.14 | 1.64 ± 0.93 | 1.74 ± 1.40 | 1.57 ± 1.06 |
| *Tnf* | 1.05 ± 0.40 | 1.03 ± 0.29 | 1.25 ± 0.43 | 1.24 ± 0.63 | 1.26 ± 0.50 | 1.34 ± 0.67 | 1.44 ± 0.48 | 1.36 ± 0.68 |
| **Oxidative stress-related genes** | | | | | | | | |
| *Cat* | 1.00 ± 0.09 | 1.01 ± 0.14 | 1.11 ± 0.37 | 1.08 ± 0.43 | 1.05 ± 0.18 | 1.10 ± 0.32 | 1.08 ± 0.38 | 1.03 ± 0.58 |
| *Gpx1* | 1.02 ± 0.24 | 1.01 ± 0.17 | 1.02 ± 0.21 | 0.97 ± 0.23 | 1.05 ± 0.22 | 1.06 ± 0.12 | 1.07 ± 0.17 | 1.01 ± 0.37 |
| *Gpx2* | 1.02 ± 0.21 | 1.01 ± 0.14 | 1.32 ± 0.68 | 1.28 ± 0.68 | 1.17 ± 0.49 | 1.24 ± 0.60 | 1.27 ± 0.60 | 1.21 ± 0.83 |
| *Gpx4* | 1.03 ± 0.29 | 1.02 ± 0.24 | 1.04 ± 0.19 | 0.99 ± 0.12 | 0.89 ± 0.18 | 0.90 ± 0.09 | 0.96 ± 0.20 | 0.90 ± 0.35 |
| *Hmox1* | 1.01 ± 0.20 | 1.01 ± 0.16 | 1.03 ± 0.18 | 0.99 ± 0.23 | 0.83 ± 0.11 | 0.86 ± 0.17 | 1.03 ± 0.33 | 0.97 ± 0.50 |
| *Keap1* | 1.01 ± 0.11 | 1.01 ± 0.12 | 1.00 ± 0.10 | 0.95 ± 0.13 | 1.07 ± 0.40 | 1.12 ± 0.53 | 0.93 ± 0.12 | 0.86 ± 0.17 |
| *Mt1* | 1.01 ± 0.13 | 1.00 ± 0.04 | 1.12 ± 0.34 | 1.10 ± 0.45 | 0.96 ± 0.18 | 0.99 ± 0.23 | 0.93 ± 0.26 | 0.85 ± 0.26 |
| *Mt2a* | 1.07 ± 0.37 | 1.05 ± 0.31 | 0.84 ± 0.21 | 0.82 ± 0.29 | 0.76 ± 0.19 | 0.76 ± 0.15 | 0.81 ± 0.46 | 0.80 ± 0.65 |
| *Nqo1* | 1.02 ± 0.23 | 1.01 ± 0.16 | 1.06 ± 0.14 | 1.00 ± 0.12 | 0.88 ± 0.17 | 0.89 ± 0.13 | 1.03 ± 0.23 | 0.98 ± 0.41 |
| *Nfe2l2* | 1.03 ± 0.27 | 1.01 ± 0.20 | 1.06 ± 0.23 | 1.02 ± 0.25 | 0.95 ± 0.09 | 0.97 ± 0.11 | 1.09 ± 0.23 | 1.01 ± 0.34 |
| *Sod1* | 1.02 ± 0.23 | 1.01 ± 0.18 | 1.07 ± 0.32 | 1.01 ± 0.20 | 0.87 ± 0.17 | 0.88 ± 0.14 | 0.98 ± 0.18 | 0.91 ± 0.29 |
| *Sod2* | 1.02 ± 0.22 | 1.01 ± 0.17 | 1.03 ± 0.14 | 0.98 ± 0.11 | 1.04 ± 0.10 | 1.07 ± 0.13 | 1.23 ± 0.35 | 1.18 ± 0.58 |
| *Txn1* | 1.03 ± 0.26 | 1.02 ± 0.21 | 1.10 ± 0.23 | 1.04 ± 0.15 | 1.00 ± 0.19 | 1.01 ± 0.16 | 1.05 ± 0.20 | 0.98 ± 0.33 |
| **PND 77** | | | | | | | | |
| **Chemical mediators and related markers** | | | | | | | | |
| *Il1a* | 1.19 ± 0.55 | 1.25 ± 0.66 | 2.47 ± 0.76[b] | 2.32 ± 0.42[b] | 2.03 ± 0.69 | 2.32 ± 1.02 | 2.02 ± 0.65 | 2.16 ± 1.08 |
| *Il1b* | 1.06 ± 0.44 | 1.12 ± 0.63 | 1.45 ± 0.37 | 1.38 ± 0.32 | 2.29 ± 1.49 | 2.47 ± 1.65 | 1.66 ± 0.90 | 1.94 ± 1.40 |
| *Il4* | 1.02 ± 0.22 | 1.04 ± 0.32 | 1.12 ± 0.39 | 1.04 ± 0.27 | 1.25 ± 0.39 | 1.26 ± 0.36 | 1.01 ± 0.24 | 1.02 ± 0.31 |
| *Il6* | 1.25 ± 0.32 | 1.27 ± 0.38 | 1.14 ± 0.19 | 1.13 ± 0.36 | 1.09 ± 0.44 | 1.29 ± 0.78 | 1.04 ± 0.54 | 1.05 ± 0.44 |
| *Tgfb1* | 1.02 ± 0.20 | 1.05 ± 0.34 | 1.34 ± 0.51 | 1.25 ± 0.27 | 1.12 ± 0.30 | 1.24 ± 0.37 | 1.18 ± 0.24 | 1.23 ± 0.46 |
| *Tnf* | 1.03 ± 0.26 | 1.05 ± 0.35 | 1.41 ± 0.57 | 1.30 ± 0.25 | 1.23 ± 0.14 | 1.37 ± 0.28 | 1.62 ± 0.86 | 1.58 ± 0.68 |

Abbreviations: AGIQ, alpha-glycosyl isoquercitrin; *Cat*, catalase; *Gapdh*, glyceraldehyde-3-phosphate dehydrogenase; *Gpx1*, glutathione peroxidase 1; *Gpx2*, glutathione peroxidase 2; *Gpx4*, glutathione peroxidase 4; *Hmox1*, heme oxygenase 1; *Hprt1*, hypoxanthine phosphoribosyltransferase 1; *Il1a*, interleukin 1 alpha; *Il1b*, interleukin 1 beta; *Il4*, interleukin 4; *Il6*, interleukin 6; *Keap1*, Kelch-like ECH-associated protein 1; LPS, lipopolysaccharides; *Mt1*, metallothionein 1; *Mt2a*, metallothionein 2A; *Nfe2l2*, nuclear factor, erythroid 2-like 2 (also known as NRF2: nuclear factor erythroid 2-related factor 2); *Nfkb1*, nuclear factor kappa B subunit 1; *Nqo1*, NAD(P)H quinone dehydrogenase 1; *Sod1*, superoxide dismutase 1; *Sod2*, superoxide dismutase 2; *Tgfb1*, transforming growth factor, beta 1; *Tnf*, tumor necrosis factor; *Txn1*, thioredoxin 1.

Data are expressed as the mean ± SD. N = 6/group.

[a] $P < 0.05$.

[b] $P < 0.01$, significantly different from the controls by Student's *t*-test or Aspin–Welch's *t*-test.

[c] $P < 0.05$.

[d] $P < 0.01$, significantly different from the LPS alone by Dunnett's test or Aspin–Welch's *t*-test with Bonferroni correction.

immature granule cells [53], remained unchanged. TUNEL$^+$ apoptotic cells increased in the SGZ but not in the GCL, which suggested that neonatal LPS treatment targeted the differentiation of immature granule cells in the SGZ, inducing apoptotic death and resulting in reduced mature granule cell populations at weaning. By contrast, at PND 77, LPS alone decreased the populations of DCX$^+$ and TUBB3$^+$ cells and reduced the transcript level of *Tubb3*, whereas the numbers of TBR2$^+$ cells, which represent type-2b NPCs [11], remained unchanged and NeuN$^+$ cell numbers recovered to the control level. These results suggested that neonatal LPS treatment decreased the numbers of type-3 NPCs and immature granule cells during adulthood. The increase in PCNA$^+$ SGZ cells observed at PND 77 suggested the compensatory proliferation of granule cell lineages. In the literature, the cell populations in granule cell lineages targeted by developmental LPS treatment are not consistent across the timing of LPS treatment or analysis, and effects in different subpopulations have been reported [5]. Differences in the targeted cells

**Table 2**
Transcript-level expression changes of neurogenesis-related genes in the hippocampal dentate gyrus in male pups on PND 21.

| | Control | | LPS alone | | LPS + 0.25% AGIQ | | LPS + 0.5% AGIQ | |
|---|---|---|---|---|---|---|---|---|
| | Relative transcript level normalized to | | | | | | | |
| | *Gapdh* | *Hprt1* | *Gapdh* | *Hprt1* | *Gapdh* | *Hprt1* | *Gapdh* | *Hprt1* |
| **Granule cell lineage markers** | | | | | | | | |
| *Nes* | 1.02 ± 0.21 | 1.04 ± 0.34 | 1.23 ± 0.30 | 1.15 ± 0.35 | 1.11 ± 0.33 | 1.03 ± 0.37 | 0.98 ± 0.11 | 1.02 ± 0.19 |
| *Sox2* | 1.05 ± 0.42 | 1.04 ± 0.34 | 0.95 ± 0.28 | 0.89 ± 0.20 | 0.91 ± 0.37 | 0.90 ± 0.29 | 0.90 ± 0.15 | 0.82 ± 0.11 |
| *Eomes* | 1.02 ± 0.21 | 1.02 ± 0.22 | 1.26 ± 0.50 | 1.23 ± 0.57 | 1.24 ± 0.52 | 1.30 ± 0.62 | 1.44 ± 0.18 | 1.32 ± 0.28 |
| *Dcx* | 1.01 ± 0.18 | 1.03 ± 0.28 | 1.16 ± 0.28 | 1.13 ± 0.36 | 0.94 ± 0.21 | 0.98 ± 0.31 | 1.31 ± 0.21 | 1.21 ± 0.32 |
| *Dpysl3* | 1.01 ± 0.14 | 1.02 ± 0.20 | 1.02 ± 0.15 | 0.98 ± 0.14 | 1.02 ± 0.12 | 1.06 ± 0.25 | 1.25 ± 0.22 | 1.17 ± 0.38 |
| *Tubb3* | 1.01 ± 0.19 | 1.01 ± 0.18 | 0.83 ± 0.11 | 0.80 ± 0.17 | 0.95 ± 0.11 | 0.98 ± 0.24 | 0.99 ± 0.20 | 0.94 ± 0.38 |
| *Rbfox3* | 1.01 ± 0.12 | 1.00 ± 0.11 | 0.70 ± 0.16[b] | 0.65 ± 0.15[b] | 1.01 ± 0.12[d] | 0.93 ± 0.18[c] | 0.94 ± 0.12[c] | 0.97 ± 0.13[d] |
| **Cell proliferation marker** | | | | | | | | |
| *Pcna* | 1.03 ± 0.26 | 1.03 ± 0.24 | 0.99 ± 0.13 | 0.94 ± 0.12 | 0.94 ± 0.21 | 0.94 ± 0.14 | 0.93 ± 0.09 | 0.85 ± 0.17 |
| **Cell cycle-related genes** | | | | | | | | |
| *Ccnd1* | 1.01 ± 0.15 | 1.00 ± 0.09 | 1.04 ± 0.15 | 1.00 ± 0.23 | 0.97 ± 0.15 | 1.01 ± 0.28 | 1.00 ± 0.16 | 0.93 ± 0.31 |
| *Ccnd2* | 1.02 ± 0.19 | 1.02 ± 0.24 | 1.29 ± 0.24 | 1.24 ± 0.26 | 1.13 ± 0.18 | 1.18 ± 0.35 | 1.26 ± 0.23 | 1.16 ± 0.27 |
| *Cdk1* | 1.04 ± 0.37 | 1.04 ± 0.32 | 1.32 ± 0.20 | 1.28 ± 0.32 | 1.13 ± 0.67 | 1.15 ± 0.67 | 0.76 ± 0.12 | 0.70 ± 0.19 |
| *Cdk2* | 1.01 ± 0.12 | 1.01 ± 0.15 | 1.07 ± 0.17 | 1.04 ± 0.31 | 0.98 ± 0.05 | 1.01 ± 0.17 | 0.93 ± 0.19 | 0.88 ± 0.34 |
| *Chek1* | 1.06 ± 0.36 | 1.06 ± 0.39 | 1.35 ± 0.83 | 1.37 ± 1.07 | 0.91 ± 0.45 | 0.96 ± 0.52 | 0.79 ± 0.23 | 0.72 ± 0.23 |
| *Tp53* | 1.01 ± 0.14 | 1.01 ± 0.16 | 1.06 ± 0.36 | 1.06 ± 0.54 | 0.91 ± 0.15 | 0.96 ± 0.29 | 1.04 ± 0.18 | 0.97 ± 0.31 |
| **Apoptosis-related genes** | | | | | | | | |
| *Bak1* | 1.01 ± 0.18 | 1.01 ± 0.18 | 0.96 ± 0.23 | 0.94 ± 0.33 | 0.89 ± 0.13 | 0.93 ± 0.23 | 0.99 ± 0.27 | 0.93 ± 0.44 |
| *Bax* | 1.01 ± 0.19 | 1.01 ± 0.17 | 1.02 ± 0.13 | 0.97 ± 0.12 | 0.89 ± 0.13 | 0.91 ± 0.17 | 0.96 ± 0.14 | 0.89 ± 0.27 |
| *Bcl2* | 1.02 ± 0.18 | 1.01 ± 0.18 | 0.98 ± 0.30 | 0.97 ± 0.39 | 0.87 ± 0.20 | 0.92 ± 0.31 | 0.98 ± 0.21 | 0.92 ± 0.36 |
| *Casp1* | 1.01 ± 0.18 | 1.01 ± 0.18 | 0.94 ± 0.17 | 0.91 ± 0.29 | 0.94 ± 0.12 | 0.97 ± 0.18 | 1.02 ± 0.20 | 0.95 ± 0.35 |
| *Casp3* | 1.11 ± 0.52 | 1.15 ± 0.62 | 2.82 ± 2.02 | 2.87 ± 2.43 | 1.75 ± 0.75 | 1.78 ± 0.80 | 0.98 ± 0.41 | 0.94 ± 0.47 |
| *Casp6* | 1.04 ± 0.36 | 1.07 ± 0.46 | 1.66 ± 0.83 | 1.69 ± 1.20 | 1.51 ± 0.43 | 1.57 ± 0.61 | 1.26 ± 0.37 | 1.18 ± 0.48 |
| *Casp8* | 1.00 ± 0.08 | 1.00 ± 0.07 | 1.05 ± 0.28 | 1.04 ± 0.47 | 0.97 ± 0.26 | 1.01 ± 0.34 | 1.10 ± 0.25 | 1.00 ± 0.26 |
| *Casp9* | 1.02 ± 0.19 | 1.02 ± 0.19 | 0.85 ± 0.10 | 0.82 ± 0.16 | 0.78 ± 0.06 | 0.80 ± 0.17 | 0.87 ± 0.24 | 0.81 ± 0.32 |
| *Casp12* | 1.05 ± 0.39 | 1.03 ± 0.30 | 1.13 ± 0.38 | 1.10 ± 0.47 | 1.05 ± 0.38 | 1.11 ± 0.48 | 1.25 ± 0.33 | 1.15 ± 0.37 |
| **GABAergic interneuron markers** | | | | | | | | |
| *Calb1* | 1.01 ± 0.19 | 1.03 ± 0.26 | 0.86 ± 0.20 | 0.81 ± 0.14 | 0.88 ± 0.34 | 0.91 ± 0.40 | 1.35 ± 0.35[c] | 1.24 ± 0.37 |
| *Calb2* | 1.13 ± 0.65 | 1.14 ± 0.67 | 1.06 ± 0.71 | 0.96 ± 0.58 | 0.85 ± 0.16 | 0.89 ± 0.27 | 0.95 ± 0.40 | 0.89 ± 0.41 |
| *Pvalb* | 1.05 ± 0.36 | 1.04 ± 0.30 | 0.69 ± 0.19 | 0.66 ± 0.17[a] | 0.69 ± 0.11 | 0.70 ± 0.08 | 0.85 ± 0.27 | 0.81 ± 0.38 |
| *Reln* | 1.01 ± 0.13 | 1.02 ± 0.23 | 0.92 ± 0.24 | 0.89 ± 0.28 | 0.75 ± 0.15 | 0.78 ± 0.22 | 1.03 ± 0.30 | 0.97 ± 0.46 |
| *Sst* | 1.06 ± 0.40 | 1.05 ± 0.35 | 0.99 ± 0.17 | 0.95 ± 0.24 | 0.83 ± 0.07 | 0.86 ± 0.18 | 1.00 ± 0.32 | 0.95 ± 0.47 |
| **Cholinergic receptors** | | | | | | | | |
| *Chrm1* | 1.01 ± 0.14 | 1.01 ± 0.19 | 0.89 ± 0.09 | 0.83 ± 0.13 | 0.88 ± 0.11 | 0.81 ± 0.17 | 0.92 ± 0.08 | 0.98 ± 0.05 |
| *Chrm2* | 1.02 ± 0.20 | 1.03 ± 0.25 | 1.12 ± 0.28 | 1.03 ± 0.17 | 1.31 ± 0.26 | 1.21 ± 0.34 | 0.91 ± 0.27 | 0.95 ± 0.20 |
| *Chrna7* | 1.02 ± 0.21 | 1.01 ± 0.15 | 1.01 ± 0.14 | 0.94 ± 0.10 | 1.12 ± 0.11 | 1.02 ± 0.11 | 1.11 ± 0.20 | 1.18 ± 0.16[d] |
| *Chrnb2* | 1.00 ± 0.09 | 1.01 ± 0.19 | 1.00 ± 0.09 | 0.93 ± 0.13 | 1.10 ± 0.09 | 1.01 ± 0.19 | 0.95 ± 0.13 | 1.01 ± 0.06 |
| **Dopaminergic receptor** | | | | | | | | |
| *Drd2* | 1.03 ± 0.28 | 1.04 ± 0.34 | 1.18 ± 0.20 | 1.10 ± 0.18 | 1.61 ± 0.94 | 1.43 ± 0.73 | 0.69 ± 0.10[d] | 0.73 ± 0.08[c] |
| **Glutamatergic receptors and glutamate transporters** | | | | | | | | |
| *Gria1* | 1.00 ± 0.08 | 1.01 ± 0.14 | 0.92 ± 0.19 | 0.90 ± 0.30 | 0.74 ± 0.19 | 0.77 ± 0.28 | 1.10 ± 0.40 | 1.05 ± 0.57 |
| *Gria2* | 1.00 ± 0.10 | 1.01 ± 0.17 | 0.83 ± 0.13[a] | 0.79 ± 0.18 | 0.71 ± 0.18 | 0.74 ± 0.23 | 1.05 ± 0.21 | 0.98 ± 0.34 |
| *Gria3* | 1.01 ± 0.16 | 1.02 ± 0.18 | 0.85 ± 0.14 | 0.83 ± 0.25 | 0.71 ± 0.16 | 0.73 ± 0.22 | 0.99 ± 0.31 | 0.94 ± 0.44 |
| *Grin2a* | 1.03 ± 0.26 | 1.03 ± 0.28 | 0.82 ± 0.24 | 0.81 ± 0.36 | 0.78 ± 0.15 | 0.80 ± 0.22 | 0.96 ± 0.31 | 0.92 ± 0.49 |
| *Grin2b* | 1.01 ± 0.18 | 1.02 ± 0.21 | 0.80 ± 0.16 | 0.78 ± 0.25 | 0.73 ± 0.14 | 0.76 ± 0.23 | 1.04 ± 0.36 | 0.99 ± 0.54 |
| *Grin2d* | 1.02 ± 0.21 | 1.01 ± 0.18 | 0.93 ± 0.14 | 0.86 ± 0.10 | 1.10 ± 0.25 | 1.00 ± 0.18 | 1.00 ± 0.34 | 1.04 ± 0.26 |
| *Slc17a7* | 1.02 ± 0.20 | 1.03 ± 0.25 | 0.97 ± 0.26 | 0.93 ± 0.28 | 1.00 ± 0.23 | 1.04 ± 0.35 | 1.14 ± 0.23 | 1.07 ± 0.42 |
| **Synaptic plasticity-related genes** | | | | | | | | |
| *Arc* | 1.03 ± 0.27 | 1.03 ± 0.27 | 0.97 ± 0.31 | 0.91 ± 0.29 | 0.88 ± 0.16 | 0.81 ± 0.18 | 0.72 ± 0.29 | 0.77 ± 0.32 |
| *Fos* | 1.01 ± 0.16 | 1.01 ± 0.14 | 0.93 ± 0.11 | 0.87 ± 0.10 | 1.02 ± 0.11 | 0.94 ± 0.17 | 0.82 ± 0.16 | 0.87 ± 0.14 |
| *Jun* | 1.03 ± 0.29 | 1.04 ± 0.33 | 0.82 ± 0.17 | 0.76 ± 0.19 | 1.02 ± 0.28 | 0.95 ± 0.34 | 1.02 ± 0.22 | 1.08 ± 0.21 |
| *Mapk1* | 1.03 ± 0.29 | 1.04 ± 0.32 | 0.76 ± 0.15 | 0.72 ± 0.21 | 0.97 ± 0.22 | 0.91 ± 0.32 | 1.00 ± 0.36 | 1.08 ± 0.45 |
| *Mapk3* | 1.35 ± 1.01 | 1.35 ± 0.90 | 0.72 ± 0.44 | 0.68 ± 0.41 | 1.12 ± 0.80 | 1.09 ± 0.92 | 1.41 ± 1.03 | 1.58 ± 1.27 |
| *Ptgs2* | 1.04 ± 0.29 | 1.03 ± 0.29 | 0.77 ± 0.10 | 0.71 ± 0.08[a] | 1.16 ± 0.28[d] | 1.07 ± 0.33[c] | 1.12 ± 0.13[c] | 1.19 ± 0.18[d] |
| **Neurotrophic factor-related genes** | | | | | | | | |
| *Bdnf* | 1.01 ± 0.11 | 1.02 ± 0.21 | 0.93 ± 0.29 | 0.92 ± 0.41 | 0.93 ± 0.13 | 0.97 ± 0.24 | 1.52 ± 0.58[d] | 1.46 ± 0.84[c] |
| *Cntf* | 1.01 ± 0.14 | 1.01 ± 0.17 | 0.99 ± 0.31 | 0.95 ± 0.28 | 1.08 ± 0.13 | 1.11 ± 0.21 | 1.80 ± 0.48 | 1.70 ± 0.69 |
| *Ntrk1* | 1.11 ± 0.50 | 1.10 ± 0.49 | 1.05 ± 0.36 | 1.02 ± 0.39 | 1.64 ± 0.62 | 1.70 ± 0.75 | 1.37 ± 0.32 | 1.27 ± 0.38 |
| *Ntrk2* | 1.01 ± 0.15 | 1.01 ± 0.14 | 0.91 ± 0.17 | 0.88 ± 0.23 | 0.81 ± 0.09 | 0.84 ± 0.19 | 0.90 ± 0.23 | 0.85 ± 0.36 |
| **DNA repair-related genes** | | | | | | | | |
| *Apex1* | 1.04 ± 0.36 | 1.03 ± 0.28 | 0.95 ± 0.05 | 0.91 ± 0.18 | 0.87 ± 0.10 | 0.89 ± 0.14 | 0.93 ± 0.09 | 0.86 ± 0.21 |
| *Brip1* | 1.01 ± 0.16 | 1.01 ± 0.19 | 0.93 ± 0.35 | 0.91 ± 0.43 | 0.90 ± 0.25 | 0.94 ± 0.33 | 0.96 ± 0.24 | 0.87 ± 0.20 |
| *Ercc1* | 1.01 ± 0.18 | 1.02 ± 0.20 | 0.95 ± 0.13 | 0.92 ± 0.22 | 0.78 ± 0.11 | 0.81 ± 0.21 | 0.95 ± 0.16 | 0.90 ± 0.34 |
| *Ogg1* | 1.01 ± 0.16 | 1.01 ± 0.17 | 0.99 ± 0.08 | 0.95 ± 0.21 | 0.93 ± 0.11 | 0.97 ± 0.24 | 1.03 ± 0.20 | 0.96 ± 0.30 |

Abbreviations: AGIQ, alpha-glycosyl isoquercitrin; *Apex1*, apurinic/apyrimidinic endodeoxyribonuclease 1; *Arc*, activity-regulated cytoskeleton-associated protein; *Bak1*, BCL2-antagonist/killer 1; *Bax*, BCL2 associated X, apoptosis regulator; *Bcl2*, BCL2, apoptosis regulator; *Bdnf*, brain-derived neurotrophic factor; *Brip1*, BRCA1 interacting protein C-terminal helicase 1; *Calb1*, calbindin 1 (also known as calbindin-D-28K); *Calb2*, calbindin 2 (also known as calbindin-D-29K and calretinin); *Casp1*, caspase 1; *Casp3*, caspase 3; *Casp6*, caspase 6; *Casp8*, caspase 8; *Casp9*, caspase 9; *Casp12*, caspase 12; *Ccnd1*, cyclin D1; *Ccnd2*, cyclin D2; *Cdk1*, cyclin-dependent kinase 1; *Cdk2*, cyclin-dependent kinase 2; *Chek1*, checkpoint kinase 1; *Chrm1*, cholinergic receptor, muscarinic 1; *Chrm2*, cholinergic receptor, muscarinic 2; *Chrna7*, cholinergic receptor nicotinic alpha 7 subunit; *Chrnb2*, cholinergic receptor nicotinic beta 2 subunit; *Cntf*, ciliary neurotrophic factor; *Dcx*,

doublecortin; *Dpysl3,* dihydropyrimidinase-like 3 (also known as TUC4: TOAD-64/Ulip/CRMP protein 4b); *Drd2*, dopamine receptor D2; *Eomes*, eomesodermin (also known as TBR2: T-box brain protein 2); *Ercc1*, ERCC excision repair 1, endonuclease non-catalytic subunit; *Fos*, Fos proto-oncogene, AP-1 transcription factor subunit; *Gapdh*, glyceraldehyde-3-phosphate dehydrogenase; *Gria1*, glutamate ionotropic receptor AMPA type subunit 1; *Gria2*, glutamate ionotropic receptor AMPA type subunit 2; *Gria3*, glutamate ionotropic receptor AMPA type subunit 3; *Grin2a*, glutamate ionotropic receptor NMDA type subunit 2A; *Grin2b*, glutamate ionotropic receptor NMDA type subunit 2B; *Grin2d*, glutamate ionotropic receptor NMDA type subunit 2D; *Hprt1*, hypoxanthine phosphoribosyltransferase 1; *Jun*, Jun proto-oncogene, AP-1 transcription factor subunit; LPS, lipopolysaccharides; *Mapk1*, mitogen activated protein kinase 1; *Mapk3*, mitogen activated protein kinase 3; *Nes*, nestin; *Ntrk1*, neurotrophic receptor tyrosine kinase 1; *Ntrk2*, neurotrophic receptor tyrosine kinase 2 (also known as TrkB: tropomyosin receptor kinase B); *Ogg1*, 8-oxoguanine DNA glycosylase; *Pcna*, proliferating cell nuclear antigen; *Ptgs2*, prostaglandin-endoperoxide synthase 2 (also known as COX2: cyclooxygenase-2); *Pvalb*, parvalbumin; *Rbfox3*, RNA binding fox-1 homolog 3 (also known as NeuN); *Reln*, reelin; *Slc17a7*, solute carrier family 17 member 7; *Sox2*, SRY-box transcription factor 2; *Sst*, somatostatin; *Tp53*, tumor protein p53; *Tubb3*, tubulin, beta 3 class III.

Data are expressed as the mean ± SD. N = 6/group.

[a] $P < 0.05$.

[b] $P < 0.01$, significantly different from the controls by Student's *t*-test or Aspin-Welch's *t*-test.

[c] $P < 0.05$.

[d] $P < 0.01$, significantly different from the LPS alone by Dunnett's test or Aspin–Welch's *t*-test with Bonferroni correction.

**Table 3**

Transcript-level expression changes of neurogenesis-related genes in the hippocampal dentate gyrus in male pups on PND 77.

| | Control | | LPS alone | | LPS + 0.25% AGIQ | | LPS + 0.5% AGIQ | |
|---|---|---|---|---|---|---|---|---|
| | Relative transcript level normalized to | | | | | | | |
| | *Gapdh* | *Hprt1* | *Gapdh* | *Hprt1* | *Gapdh* | *Hprt1* | *Gapdh* | *Hprt1* |
| **Granule cell lineage markers** | | | | | | | | |
| *Nes* | 1.01 ± 0.18 | 0.91 ± 0.23 | 1.20 ± 0.17 | 1.05 ± 0.27 | 1.23 ± 0.27 | 1.22 ± 0.33 | 1.21 ± 0.23 | 1.14 ± 0.47 |
| *Sox2* | 1.01 ± 0.16 | 1.01 ± 0.15 | 1.11 ± 0.25 | 1.09 ± 0.36 | 1.03 ± 0.22 | 1.14 ± 0.31 | 0.96 ± 0.22 | 0.99 ± 0.29 |
| *Eomes* | 1.01 ± 0.15 | 1.01 ± 0.13 | 1.10 ± 0.32 | 1.03 ± 0.09 | 0.91 ± 0.15 | 1.02 ± 0.28 | 1.01 ± 0.32 | 1.00 ± 0.29 |
| *Dcx* | 1.01 ± 0.15 | 1.03 ± 0.30 | 0.95 ± 0.14 | 1.05 ± 0.30 | 0.95 ± 0.19 | 1.04 ± 0.19 | 1.00 ± 0.19 | 1.03 ± 0.33 |
| *Tubb3* | 1.01 ± 0.13 | 1.01 ± 0.19 | 0.66 ± 0.24[a] | 0.65 ± 0.30[a] | 0.95 ± 0.15[b] | 1.05 ± 0.19 | 1.12 ± 0.21[c] | 1.17 ± 0.43[b] |
| *Dpysl3* | 1.00 ± 0.10 | 1.03 ± 0.26 | 1.13 ± 0.42 | 1.06 ± 0.22 | 0.94 ± 0.18 | 1.04 ± 0.19 | 1.00 ± 0.27 | 1.06 ± 0.25 |
| *Rbfox3* | 1.01 ± 0.14 | 1.03 ± 0.26 | 1.18 ± 0.37 | 1.11 ± 0.22 | 0.90 ± 0.20 | 0.98 ± 0.17 | 0.90 ± 0.13 | 0.91 ± 0.19 |
| **GABAergic interneuron markers** | | | | | | | | |
| *Calb1* | 1.01 ± 0.19 | 1.03 ± 0.25 | 1.28 ± 0.34 | 1.23 ± 0.38 | 1.17 ± 0.23 | 1.29 ± 0.32 | 1.00 ± 0.19 | 1.02 ± 0.27 |
| *Calb2* | 1.00 ± 0.08 | 1.01 ± 0.16 | 1.14 ± 0.21 | 1.10 ± 0.30 | 0.94 ± 0.21 | 1.05 ± 0.30 | 1.05 ± 0.22 | 1.13 ± 0.23 |
| *Pvalb* | 1.02 ± 0.23 | 1.02 ± 0.20 | 1.23 ± 0.21 | 1.11 ± 0.29 | 0.99 ± 0.19 | 0.91 ± 0.29 | 1.11 ± 0.34 | 0.95 ± 0.42 |
| *Reln* | 1.01 ± 0.12 | 1.01 ± 0.13 | 1.00 ± 0.17 | 0.96 ± 0.18 | 1.07 ± 0.14 | 1.20 ± 0.29 | 0.98 ± 0.07 | 1.03 ± 0.29 |
| *Sst* | 1.02 ± 0.22 | 1.03 ± 0.25 | 1.08 ± 0.30 | 1.03 ± 0.29 | 1.11 ± 0.11 | 1.22 ± 0.22 | 0.87 ± 0.17 | 0.91 ± 0.29 |
| **Cholinergic receptors** | | | | | | | | |
| *Chrm1* | 1.01 ± 0.15 | 1.02 ± 0.20 | 1.22 ± 0.28 | 1.17 ± 0.22 | 0.93 ± 0.19 | 1.01 ± 0.17 | 0.92 ± 0.18 | 0.93 ± 0.16 |
| *Chrm2* | 1.04 ± 0.31 | 1.04 ± 0.32 | 0.97 ± 0.43 | 0.90 ± 0.26 | 0.96 ± 0.23 | 1.04 ± 0.21 | 1.36 ± 0.57 | 1.47 ± 0.92 |
| *Chrna7* | 1.03 ± 0.28 | 1.07 ± 0.40 | 1.21 ± 0.37 | 1.13 ± 0.17 | 0.82 ± 0.15[b] | 0.90 ± 0.16 | 0.95 ± 0.10 | 1.05 ± 0.28 |
| *Chrnb2* | 1.01 ± 0.18 | 1.03 ± 0.26 | 1.09 ± 0.43 | 1.02 ± 0.23 | 1.00 ± 0.19 | 1.09 ± 0.19 | 1.12 ± 0.17 | 1.17 ± 0.39 |
| **Dopaminergic receptors** | | | | | | | | |
| *Drd2* | 1.07 ± 0.47 | 1.06 ± 0.40 | 1.17 ± 0.29 | 1.11 ± 0.19 | 1.35 ± 0.59 | 1.45 ± 0.41 | 1.24 ± 0.56 | 1.34 ± 0.86 |
| **Glutamatergic receptors** | | | | | | | | |
| *Gria1* | 1.02 ± 0.21 | 1.04 ± 0.28 | 1.30 ± 0.38 | 1.23 ± 0.21 | 0.90 ± 0.21[b] | 0.97 ± 0.18 | 0.96 ± 0.15 | 0.97 ± 0.19 |
| *Gria2* | 1.03 ± 0.24 | 1.06 ± 0.35 | 1.30 ± 0.43 | 1.23 ± 0.24 | 0.83 ± 0.22[b] | 0.90 ± 0.20 | 0.87 ± 0.13[b] | 0.91 ± 0.29 |
| *Gria3* | 1.02 ± 0.21 | 1.03 ± 0.25 | 1.27 ± 0.42 | 1.20 ± 0.25 | 0.87 ± 0.18[b] | 0.95 ± 0.17 | 0.86 ± 0.16[b] | 0.90 ± 0.30 |
| *Grin2a* | 1.02 ± 0.20 | 1.03 ± 0.24 | 1.27 ± 0.33 | 1.21 ± 0.25 | 0.97 ± 0.24 | 1.05 ± 0.17 | 1.00 ± 0.28 | 0.97 ± 0.06 |
| *Grin2b* | 1.02 ± 0.21 | 1.04 ± 0.29 | 1.40 ± 0.50 | 1.31 ± 0.24 | 1.02 ± 0.24 | 1.11 ± 0.23 | 1.02 ± 0.23 | 1.02 ± 0.21 |
| **Synaptic plasticity-related genes** | | | | | | | | |
| *Arc* | 1.05 ± 0.31 | 1.04 ± 0.31 | 1.55 ± 0.34[a] | 1.49 ± 0.37[a] | 0.96 ± 0.23[c] | 1.05 ± 0.25[b] | 0.98 ± 0.24[c] | 0.97 ± 0.16[c] |
| *Fos* | 1.01 ± 0.15 | 1.02 ± 0.23 | 1.12 ± 0.21 | 1.08 ± 0.24 | 1.04 ± 0.19 | 1.13 ± 0.18 | 1.16 ± 0.33 | 1.21 ± 0.53 |
| *Mapk1* | 1.04 ± 0.28 | 1.06 ± 0.36 | 1.20 ± 0.39 | 1.13 ± 0.21 | 0.95 ± 0.10 | 1.06 ± 0.26 | 1.03 ± 0.14 | 1.05 ± 0.17 |
| *Mapk3* | 1.02 ± 0.21 | 1.05 ± 0.35 | 1.35 ± 0.42 | 1.26 ± 0.16 | 0.96 ± 0.15 | 1.08 ± 0.30 | 0.98 ± 0.17 | 1.00 ± 0.27 |
| **Neurotrophic factor-related genes** | | | | | | | | |
| *Bdnf* | 1.01 ± 0.14 | 1.03 ± 0.16 | 1.02 ± 0.23 | 0.97 ± 0.12 | 0.87 ± 0.16 | 0.95 ± 0.13 | 0.83 ± 0.17 | 0.85 ± 0.25 |
| *Cntf* | 1.00 ± 0.11 | 1.02 ± 0.19 | 1.15 ± 0.13[a] | 1.12 ± 0.29 | 1.16 ± 0.16 | 1.27 ± 0.19 | 1.17 ± 0.20 | 1.13 ± 0.32 |
| *Ntrk1* | 1.09 ± 0.08 | 1.06 ± 0.10 | 1.11 ± 0.20 | 1.09 ± 0.14 | 0.92 ± 0.20 | 1.00 ± 0.11 | 0.88 ± 0.31 | 1.06 ± 0.31 |
| *Ntrk2* | 1.01 ± 0.17 | 1.03 ± 0.18 | 1.19 ± 0.32 | 1.14 ± 0.31 | 0.78 ± 0.20[b] | 0.86 ± 0.20 | 1.01 ± 0.26 | 1.05 ± 0.33 |

Abbreviations: AGIQ, alpha-glycosyl isoquercitrin; *Arc*, activity-regulated cytoskeleton-associated protein; *Bdnf*, brain-derived neurotrophic factor; *Calb1*, calbindin 1 (also known as calbindin-D-28K); *Calb2*, calbindin 2 (also known as calbindin-D-29K and calretinin); *Chrm1*, cholinergic receptor, muscarinic 1; *Chrm2*, cholinergic receptor, muscarinic 2; *Chrna7*, cholinergic receptor nicotinic alpha 7 subunit; *Chrnb2*, cholinergic receptor nicotinic beta 2 subunit; *Cntf*, ciliary neurotrophic factor; *Dcx*, doublecortin; *Dpysl3,* dihydropyrimidinase-like 3 (also known as TUC4: TOAD-64/Ulip/CRMP protein 4b); *Drd2*, dopamine receptor D2; *Eomes*, eomesodermin (also known as TBR2: T-box brain protein 2); *Fos*, Fos proto-oncogene, AP-1 transcription factor subunit; *Gapdh*, glyceraldehyde-3-phosphate dehydrogenase; *Gria1*, glutamate ionotropic receptor AMPA type subunit 1; *Gria2*, glutamate ionotropic receptor AMPA type subunit 2; *Gria3*, glutamate ionotropic receptor AMPA type subunit 3; *Grin2a*, glutamate ionotropic receptor NMDA type subunit 2A; *Grin2b*, glutamate ionotropic receptor NMDA type subunit 2B; *Hprt1*, hypoxanthine phosphoribosyltransferase 1; LPS, lipopolysaccharides; *Mapk1*, mitogen activated protein kinase 1; *Mapk3*, mitogen activated protein kinase 3; *Nes*, nestin; *Ntrk1*, neurotrophic receptor tyrosine kinase 1; *Ntrk2*, neurotrophic receptor tyrosine kinase 2 (also known as TrkB: tropomyosin receptor kinase B); *Pvalb*, parvalbumin; *Rbfox3*, RNA binding fox-1 homolog 3 (also known as NeuN); *Reln*, reelin; *Sox2*, SRY-box transcription factor 2; *Sst*, somatostatin; *Tubb3*, tubulin, beta 3 class III.

Data are expressed as the mean ± SD. N = 6/group.

[a] $P < 0.05$, significantly different from the controls by Student's *t*-test or Aspin-Welch's *t*-test.

[b] $P < 0.05$.

[c] $P < 0.01$, significantly different from the LPS alone by Dunnett's test or Aspin–Welch's *t*-test with Bonferroni correction.

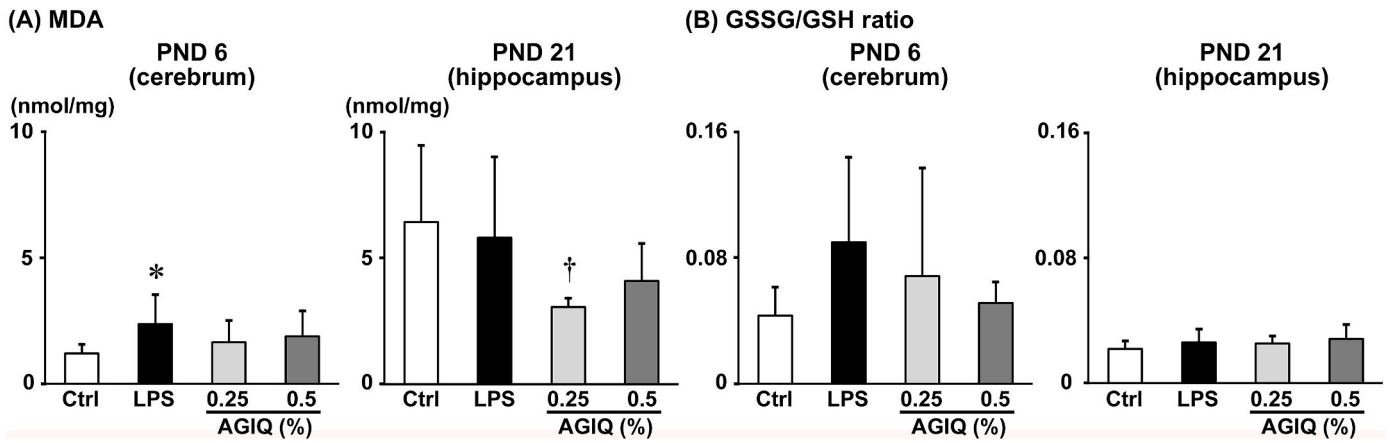


**Fig. 8.** The results of the oxidative stress measurement in the brain of male pups at postnatal day (PND) 6 and PND 21. N = 7/group. Values are expressed as the mean +SD. *$P < 0.05$, significantly different from the controls by Student's *t*-test or Aspin–Welch's *t*-test. †$P < 0.05$, significantly different from the LPS alone by Dunnett's test or Aspin–Welch's *t*-test with Bonferroni correction.

reported across different studies may reflect the complex effects of concurrent, long-lasting, progressive damage and the compensatory neurogenic responses following developmental LPS treatment. However, LPS-induced pro-inflammatory responses and oxidative stress were generally terminated by PND 21 in the present study. Maternal LPS treatment has been reported to damage the molecular mechanisms that control development, causing long-term or irreversible changes in function [54]. LPS may have caused the progressive disruption of neurogenesis due to impaired developmental processes in the neurogenic regulatory system during early postnatal life.

In the current study, LPS-induced disruption in neurogenesis at both PND 21 and PND 77 were restored by AGIQ treatment. AGIQ treatment started before LPS treatment rescued almost all early neuroinflammation and oxidative stress caused by LPS treatment, likely through antioxidant effects, and prevented subsequent effects on neurogenesis and behavior. In accordance with the present study results, the maternal administration of the antioxidant N-acetyl-L-cysteine or zinc salts starting before LPS treatment inhibited the production of TNF-α, IL-6, and IL-10 and prevented the development of local inflammation in the fetal brain, which abolished the long-term negative consequences of inflammation [55,56].

In the present study, AGIQ treatment increased the populations of granule cells immunoreactive for the IEG protein FOS [57] or the IEG regulator p-ERK1/2 [41] on PND 21. The increased expression of IEGs in hippocampal neurons plays a critical role in neuroplasticity and memory consolidation processes [58]. ERK1/2 can also be rapidly activated by phosphorylation in response to acute stimuli, inducing IEGs to participate in the facilitation of synaptic plasticity [59]. We previously reported that continuous AGIQ exposure starting during developmental stages in normal animals facilitates fear extinction learning in contextual fear conditioning tests and enhances synaptic plasticity mediated by FOS and p-ERK1/2 in the dentate gyrus and medial frontal cortex [27,28]. Therefore, continuous AGIQ treatment in this study likely exerts neuroprotective functions against LPS-induced detrimental effects, leading to the facilitation of synaptic plasticity. It is now understood that the biological actions of naturally occurring antioxidants, such as flavonoids, within the nervous system are not due to their classical antioxidant effects [60], but rather through their potential for interaction with intracellular signaling to protect vulnerable neurons, enhance existing neuronal function, stimulate neuronal regeneration, and induce neurogenesis [60,61].

We found, however, increased populations of granule cells immunoreactive for ARC, which is an IEG protein [42], or FOS following treatment with LPS alone and in both of the LPS + AGIQ groups on PND 77. We also found sustained increases or trends for increase in the transcript levels of *Il1a* and *Il1b* after treatment with LPS alone, and AGIQ treatment did not restore the expression of *Il1a* and *Il1b* compared with the LPS alone at either PND 21 or PND 77. IL-1α and IL-1β are key molecules in the inflammatory responses elicited during infection and injury. IL-1β has been shown to exert local effects on synaptic plasticity by binding to IL-1 receptors, which are expressed at high levels in the hippocampus [62]. IL-1β was found to exert variable effects on long-term potentiation at different synapse types, indicating that IL-1β has synapse-specific effects on hippocampal synaptic plasticity [62]. Although the functional role of IL-1α at synapses has not been well examined, one study reported the facilitation of long-term memory extinction by IL-1α in mice [63]. Therefore, animals that are neonatally exposed to LPS may demonstrate enhanced synaptic plasticity during the adult stage due to the sustained release of IL-1α and IL-1β. Because synaptic plasticity-related proteins on PND 77 in this study were examined in animals 90 min after the last behavioral test trials, any observed increases in $ARC^+$ or $FOS^+$ cells may be due to behavioral stimulus-related responses, as previously reported [28]. However, AGIQ treatment did not further modify the numbers of these immunoreactive cells, which suggests the spontaneous amelioration of synaptic plasticity at the adult stage after neonatal LPS treatment.

In the present study, LPS alone reduced the populations of $PVALB^+$ and $GAD67^+$ interneurons in the dentate gyrus hilus and downregulated *Pvalb* in the dentate gyrus at PND 21 compared with the controls. GABAergic interneurons have been reported to promote neurogenesis, with basket cells and axo-axonic cells suggested as probable candidates [64]. The major populations of basket cells and axo-axonic cells are $PVALB^+$ interneurons in the dentate gyrus [12], and decreased $PVALB^+$ interneuron signaling may result in the suppression of neurogenesis. We previously identified the disruption of hippocampal neurogenesis, which was associated with a decrease in $PVALB^+$ interneuron populations due to *Pvalb* promoter region hypermethylation following maternal exposure to manganese in mice [65]. These results suggested that neonatal LPS treatment may primarily target *Pvalb,* disrupting neurogenesis on PND 21. GAD67 is a rate-limiting enzyme responsible for greater than 90% of GABA production [66], and a subpopulation of GABAergic interneurons expresses this enzyme [67]. The observed decrease in $GAD67^+$ interneurons in the present study suggested that neonatal LPS treatment targets GABAergic interneurons, which may be partly due to the decrease in the $PVALB^+$ population.

In the present study, high-dose AGIQ treatment upregulated *Bdnf* in the dentate gyrus at PND 21 compared with LPS alone, although *Bdnf* levels did not change between the controls and LPS alone. High-dose AGIQ treatment also restored LPS-induced decreases in the $PVALB^+$ interneuron populations. Brain-derived neurotrophic factor (BDNF) is

produced by mature granule cells in the dentate gyrus [68] and has been reported to stimulate the maturation of $PVALB^+$ interneurons and the firing of action potentials [69]. Therefore, AGIQ treatment may have resulted in the recovery of $PVALB^+$ interneurons through the compensatory enhancement of BDNF signaling by mature granule cells, the population of which is reduced by neonatal LPS treatment.

In the USV test at PND 10 in the present study, LPS alone decreased the values of USV parameters, similar to the findings of a previous study examining neonatal LPS treatment [8], which suggested that communicative deficits were induced after the rapid induction of neuroinflammation. ASD is characterized by deficits in social communication, as previously mentioned, and immune dysregulation and neuroinflammation are important components of ASD [4]. USV involves a wide neural network, spanning from the forebrain to the brainstem [70], which suggests that LPS-induced ASD-like communicative abnormalities may be caused by acute neuroinflammation that involves broad brain areas, as observed in a previous study [8]. In the present study, AGIQ treatment abolished the decrease in USVs and suppressed hippocampal neuroinflammation during early postnatal life, which suggested an antioxidant-mediated neuroprotective effect against acute pro-inflammatory responses across broad areas of the developing brain. Similarly, during the adolescent stage, LPS alone caused a decrease in the interest in novel animals and reduced exploratory behavior, without observed reductions in locomotor activity during the social interaction test, which suggested the induction of ASD-like social deficits. High-dose AGIQ treatment recovered or showed a recovering trend for these various test parameters. Hippocampal neurogenesis is disrupted in ASD models, including LPS-induced models [5], and the present study also revealed LPS-induced disruptions in neurogenesis, which was ameliorated by AGIQ treatment during both weaning and adult stages. The brain regions implicated in this social behavior include the striatum, the CA2 region of the hippocampus, cerebral cortex, and amygdala [71]. Therefore, the antioxidant and neuroprotective effects of AGIQ treatment against LPS-induced acute pro-inflammatory responses across the developing brain regions may be critical for the prevention of ASD-like social deficits.

In the contextual fear conditioning test during the adolescent stage of this study, LPS alone showed a decreasing trend in the rate of freezing time at the fear acquisition and a decrease in the rate of freezing time at the first trial of fear extinction, which likely reflects suppressed fear acquisition. The hippocampal dentate gyrus plays a critical role in memory acquisition, and the ablation or silencing of adult-born granule cells impairs memory acquisition during contextual fear conditioning [72]. In the present study, LPS alone reduced mature granule cell populations at weaning, which suggests a causal relationship between the reduction of functionally active granule cell population and the impairment of memory acquisition. Although high-dose AGIQ treatment was effective for the recovery of mature granule cells, AGIQ treatment did not ameliorate the LPS-induced impairment in fear acquisition. However, the slope of the rate of freezing time during the fear memory extinction stage in the LPS + AGIQ groups was similar to that observed in controls, suggesting unaltered fear extinction learning ability. In addition to the hippocampal dentate gyrus, the medial prefrontal cortex and amygdala are involved in the acquisition, consolidation, maintenance, and extinction of fear memories [73], and the mechanism of AGIQ action on fear learning may involve the complex regulation of these brain regions. Similar to the adolescent stage, LPS alone reduced the rate of freezing time at the fear acquisition and also at the first trial of fear extinction in the adult stage, the latter likely reflects the suppression of fear acquisition. LPS alone also targeted type-3 NPCs and immature granule cells involved in hippocampal neurogenesis at the adult stage, suggesting a relationship between these cells and the disruption of fear memory acquisition. AGIQ treatment effectively ameliorated both fear memory acquisition and hippocampal neurogenesis, suggesting a reflection of the suppression of neuroinflammation during the early stages of LPS treatment due to the anti-inflammatory and antioxidant effects of AGIQ.

## 5. Conclusion

Neonatal LPS treatment induced acute pro-inflammatory responses in the brain that were associated with oxidative stress and triggered communicative deficits in neonatal rats. Although the neuroinflammatory profile shifted to an anti-inflammatory phenotype, LPS-exposed animals revealed disruptions in hippocampal neurogenesis at weaning and altered social interactions and fear memory deficits during the adolescent stage. During adulthood, LPS-induced neuroinflammatory responses disappeared; however, detrimental effects in neurogenesis and fear memory were sustained. Continuous AGIQ treatment, starting during late gestation, suppressed LPS-induced acute pro-inflammatory responses during infancy and prevented the expression of subsequent deficits in neurogenesis and behavior throughout the adult stage. Thus, neonatal LPS treatment induced acute and transient pro-inflammatory responses, resulting in the progression of ASD-like behaviors and disrupting hippocampal neurogenesis. AGIQ treatment may be able to ameliorate progressive changes in behaviors and neurogenesis by critically suppressing LPS-induced pro-inflammatory responses and oxidative brain damage.

## Author contribution statement

**Hiromu Okano:** Methodology, Formal analysis, Investigation, Data Curation, Writing - Original Draft, Visualization.

**Kazumi Takashima:** Methodology, Formal analysis, Investigation, Data Curation, Writing - Review & Editing.

**Yasunori Takahashi:** Investigation, Writing - Review & Editing.

**Ryota Ojiro:** Investigation, Writing - Review & Editing.

**Qian Tang:** Investigation, Writing - Review & Editing.

**Shunsuke Ozawa:** Investigation, Writing - Review & Editing.

**Bunichiro Ogawa:** Investigation, Writing - Review & Editing.

**Mihoko Koyanagi:** Resources, Writing - Review & Editing, Project administration.

**Robert R. Maronpot:** Validation, Writing - Review & Editing.

**Toshinori Yoshida:** Investigation, Writing - Review & Editing.

**Makoto Shibutani:** Conceptualization, Writing - Review & Editing, Visualization, Supervision, Funding acquisition.

## Declaration of competing interest

The authors declare that they have no known competing financial interests or personal relationships that could have appeared to influence the work reported in this paper.

Mihoko Koyanagi reports financial support was provided by San-Ei Gen FFI Inc. Robert R. Maronpot reports a relationship with Maronpot Consulting, LLC that includes: consulting or advisory.

## Acknowledgments

The authors thank Yayoi Kohno for her technical assistance in preparing the histological specimens. This work was supported by San-Ei Gen F.F.I., Inc. We thank Edanz Group (https://jp.edanz.com/ac) for editing a draft of this manuscript.

## Appendix A. Supplementary data

Supplementary data to this article can be found online at https://doi.org/10.1016/j.cbi.2021.109767.

## References


[1] H. Hagberg, P. Gressens, C. Mallard, Inflammation during fetal and neonatal life: implications for neurologic and neuropsychiatric disease in children and adults, Ann. Neurol. 71 (2012) 444–457, https://doi.org/10.1002/ANA.22620.

[2] S.L. Hyman, S.E. Levy, S.M. Myers, COUNCIL ON children with disabilities, section ON developmental and behavioral pediatrics, identification, evaluation, and management of children with autism spectrum disorder, Pediatrics 145 (2020), e20193447, https://doi.org/10.1542/PEDS.2019-3447.

[3] S.R. Sharma, X. Gonda, F.I. Tarazi, Autism spectrum disorder: classification, diagnosis and therapy, Pharmacol. Ther. 190 (2018) 91–104, https://doi.org/10.1016/j.pharmthera.2018.05.007.

[4] G. Bjørklund, K. Saad, S. Chirumbolo, J.K. Kern, D.A. Geier, M.R. Geier, M. A. Urbina, Immune dysfunction and neuroinflammation in autism spectrum disorder, Acta Neurobiol. Exp. (Wars) 76 (2017) 257–268, https://doi.org/10.21307/ANE-2017-025.

[5] E. Domínguez-Rivas, E. Ávila-Muñoz, S.W. Schwarzacher, A. Zepeda, Adult hippocampal neurogenesis in the context of lipopolysaccharide-induced neuroinflammation: a molecular, cellular and behavioral review, Brain Behav. Immun. 97 (2021) 286–302, https://doi.org/10.1016/j.bbi.2021.06.014.

[6] J.C. Corona, Role of oxidative stress and neuroinflammation in attention-deficit/hyperactivity disorder, Antioxidants 9 (2020) 1039, https://doi.org/10.3390/ANTIOX9111039.

[7] C.R.A. Batista, G.F. Gomes, E. Candelario-Jalil, B.L. Fiebich, A.C.P. de Oliveira, Lipopolysaccharide-induced neuroinflammation as a bridge to understand neurodegeneration, Int. J. Mol. Sci. 20 (2019) 2293, https://doi.org/10.3390/IJMS20092293.

[8] Y. Pang, X. Dai, A. Roller, K. Carter, I. Paul, A.J. Bhatt, R.C.S. Lin, L.-W. Fan, Early postnatal lipopolysaccharide exposure leads to enhanced neurogenesis and impaired communicative functions in rats, PLoS One 11 (2016), e0164403, https://doi.org/10.1371/JOURNAL.PONE.0164403.

[9] Z. Rusznák, W. Henskens, E. Schofield, W.S. Kim, Y. Fu, Adult neurogenesis and gliogenesis: possible mechanisms for neurorestoration, Exp. Neurobiol. 25 (2016) 103–112, https://doi.org/10.5607/EN.2016.25.3.103.

[10] R.D. Hodge, T.D. Kowalczyk, S.A. Wolf, J.M. Encinas, C. Rippey, G. Enikolopov, G. Kempermann, R.F. Hevner, Intermediate progenitors in adult hippocampal neurogenesis: tbr2 expression and coordinate regulation of neuronal output, J. Neurosci. 28 (2008) 3707–3717, https://doi.org/10.1523/JNEUROSCI.4280-07.2008.

[11] M. Sibbe, A. Kulik, GABAergic regulation of adult hippocampal neurogenesis, Mol. Neurobiol. 54 (2016) 5497–5510, https://doi.org/10.1007/S12035-016-0072-3.

[12] T.F. Freund, G. Buzsáki, Interneurons of the hippocampus, Hippocampus 6 (1996) 347–470, https://doi.org/10.1002/(sici)1098-1063(1996)6:4<347::aid-hipo1>3.0.co;2-i.

[13] I. Masiulis, S. Yun, A.J. Eisch, The interesting interplay between interneurons and adult hippocampal neurogenesis, Mol. Neurobiol. 44 (2011) 287–302, https://doi.org/10.1007/S12035-011-8207-Z.

[14] H. Cameron, B. McEwen, E. Gould, Regulation of adult neurogenesis by excitatory input and NMDA receptor activation in the dentate gyrus, J. Neurosci. 15 (1995) 4687–4692, https://doi.org/10.1523/JNEUROSCI.15-06-04687.1995.

[15] E.C. Cope, E. Gould, Adult neurogenesis, glia, and the extracellular matrix, Cell Stem Cell 24 (2019) 690–705, https://doi.org/10.1016/J.STEM.2019.03.023.

[16] Y. Fueta, Y. Sekino, S. Yoshida, Y. Kanda, S. Ueno, Prenatal exposure to valproic acid alters the development of excitability in the postnatal rat hippocampus, Neurotoxicology 65 (2018) 1–8, https://doi.org/10.1016/J.NEURO.2018.01.001.

[17] Z. Li, R. Jagadapillai, E. Gozal, G. Barnes, Deletion of semaphorin 3F in interneurons is associated with decreased GABAergic neurons, autism-like behavior, and increased oxidative stress cascades, Mol. Neurobiol. 56 (2019) 5520, https://doi.org/10.1007/S12035-018-1450-9.

[18] J. Rhee, K. Park, K.C. Kim, C.Y. Shin, C. Chung, Impaired hippocampal synaptic plasticity and enhanced excitatory transmission in a novel animal model of autism spectrum disorders with telomerase reverse Transcriptase overexpression, Mol. Cells 41 (2018) 486–494, https://doi.org/10.14348/MOLCELLS.2018.0145.

[19] T. Akiyama, T. Washino, T. Yamada, T. Koda, T. Maitani, Constituents of enzymatically modified isoquercitrin and enzymatically modified rutin (extract), Food Hyg. Saf. Sci. 41 (2000) 54–60, https://doi.org/10.3358/SHOKUEISHI.41.54.

[20] T. Makino, M. Kanemaru, S. Okuyama, R. Shimizu, H. Tanaka, H. Mizukami, Anti-allergic effects of enzymatically modified isoquercitrin (α-oligoglucosyl quercetin 3-*O*-glucoside), quercetin 3-*O*-glucoside, α-oligoglucosyl rutin, and quercetin, when administered orally to mice, J. Nat. Med. 67 (2013) 881–886, https://doi.org/10.1007/S11418-013-0760-5.

[21] Y. Kangawa, T. Yoshida, H. Abe, Y. Seto, T. Miyashita, M. Nakamura, T. Kihara, S. M. Hayashi, M. Shibutani, Anti-inflammatory effects of the selective phosphodiesterase 3 inhibitor, cilostazol, and antioxidants, enzymatically-modified isoquercitrin and α-lipoic acid, reduce dextran sulphate sodium-induced colorectal mucosal injury in mice, Exp. Toxicol. Pathol. 69 (2017) 179–186, https://doi.org/10.1016/J.ETP.2016.12.004.

[22] A. Gasparotto, F.M. Gasparotto, E.L.B. Lourenço, S. Crestani, M.E.A. Stefanello, M. J. Salvador, J.E. Da Silva-Santos, M.C.A. Marques, C.A.L. Kassuya, Antihypertensive effects of isoquercitrin and extracts from *Tropaeolum majus* L.: evidence for the inhibition of angiotensin converting enzyme, J. Ethnopharmacol. 134 (2011) 363–372, https://doi.org/10.1016/J.JEP.2010.12.026.

[23] Y. Fujii, M. Kimura, Y. Ishii, R. Yamamoto, R. Morita, S.M. Hayashi, K. Suzuki, M. Shibutani, Effect of enzymatically modified isoquercitrin on preneoplastic liver cell lesions induced by thioacetamide promotion in a two-stage hepatocarcinogenesis model using rats, Toxicology 305 (2013) 30–40, https://doi.org/10.1016/J.TOX.2013.01.002.

[24] K. Valentová, J. Vrba, M. Bancířová, J. Ulrichová, V. Křen, Isoquercitrin: pharmacology, toxicology, and metabolism, Food Chem. Toxicol. 68 (2014) 267–282, https://doi.org/10.1016/j.fct.2014.03.018.

[25] C. Tan, F. Meng, E.A. Reece, Z. Zhao, Modulation of nuclear factor-κB signaling and reduction of neural tube defects by quercetin-3-glucoside in embryos of diabetic mice, Am. J. Obstet. Gynecol. 219 (2018) 197.e1–197.e8, doi.org/10.1016/J.AJOG.2018.04.045.

[26] Z. Wu, J. Zhao, H. Xu, Y. Lyv, X. Feng, Y. Fang, Y. Xu, Maternal quercetin administration during gestation and lactation decrease endoplasmic reticulum stress and related inflammation in the adult offspring of obese female rats, Eur. J. Nutr. 53 (2014) 1669–1683, https://doi.org/10.1007/S00394-014-0673-4.

[27] R. Okada, Y. Masubuchi, T. Tanaka, K. Nakajima, S. Masuda, K. Nakamura, R. R. Maronpot, T. Yoshida, M. Koyanagi, S.M. Hayashi, M. Shibutani, Continuous exposure to α-glycosyl isoquercitrin from developmental stage facilitates fear extinction learning in rats, J. Funct. Foods 55 (2019) 312–324, https://doi.org/10.1016/J.JFF.2019.02.024.

[28] Y. Masubuchi, J. Nakahara, S. Kikuchi, H. Okano, Y. Takahashi, K. Takashima, M. Koyanagi, R.R. Maronpot, T. Yoshida, S.M. Hayashi, M. Shibutani, Continuous exposure to α-glycosyl isoquercitrin from developmental stages to adulthood is necessary for facilitating fear extinction learning in rats, J. Toxicol. Pathol. 33 (2020) 247–263, https://doi.org/10.1293/TOX.2020-0025.

[29] T. Tanaka, Y. Masubuchi, R. Okada, K. Nakajima, K. Nakamura, S. Masuda, J. Nakahara, R.R. Maronpot, T. Yoshida, M. Koyanagi, S.M. Hayashi, M. Shibutani, Ameliorating effect of postweaning exposure to antioxidant on disruption of hippocampal neurogenesis induced by developmental hypothyroidism in rats, J. Toxicol. Sci. 44 (2019) 357–372, https://doi.org/10.2131/JTS.44.357.

[30] J.L. Pawluski, S. Brummelte, C.K. Barha, T.M. Crozier, L.A.M. Galea, Effects of steroid hormones on neurogenesis in the hippocampus of the adult female rodent during the estrous cycle, pregnancy, lactation and aging, Front. Neuroendocrinol. 30 (2009) 343–357, https://doi.org/10.1016/J.YFRNE.2009.03.007.

[31] H. Akane, F. Saito, H. Yamanaka, A. Shiraki, N. Imatanaka, Y. Akahori, R. Morita, K. Mitsumori, M. Shibutani, Methacarn as a whole brain fixative for gene and protein expression analyses of specific brain regions in rats, J. Toxicol. Sci. 38 (2013) 431–443, https://doi.org/10.2131/JTS.38.431.

[32] H. Tsukamura, K. Maeda, Non-metabolic and metabolic factors causing lactational anestrus: rat models uncovering the neuroendocrine mechanism underlying the suckling-induced changes in the mother, Prog. Brain Res. 133 (2001) 187–205, https://doi.org/10.1016/S0079-6123(01)33014-5.

[33] S.B. Laffan, L.M. Posobiec, J.E. Uhl, J.D. Vidal, Species comparison of postnatal development of the female reproductive system, Birth Defects Res 110 (2018) 163–189, https://doi.org/10.1002/BDR2.1132.

[34] M. Wöhr, R.K.W. Schwarting, Maternal care, isolation-induced infant ultrasonic calling, and their relations to adult anxiety-related behavior in the rat, Behav. Neurosci. 122 (2008) 310–330, https://doi.org/10.1037/0735-7044.122.2.310.

[35] M. Shibutani, Hippocampal neurogenesis as a critical target of neurotoxicants contained in foods, Food Safety 3 (2015) 1–15, https://doi.org/10.14252/FOODSAFETYFSCJ.2014038.

[36] O. von, Bohlen und Halbach, Immunohistological markers for staging neurogenesis in adult hippocampus, Cell Tissue Res. 329 (2007) 409–420, https://doi.org/10.1007/S00441-007-0432-4.

[37] C. Gong, T.-W. Wang, H.S. Huang, J.M. Parent, Reelin regulates neuronal progenitor migration in intact and epileptic Hippocampus, J. Neurosci. 27 (2007) 1803–1811, https://doi.org/10.1523/JNEUROSCI.3111-06.2007.

[38] R.E. Iosif, C.T. Ekdahl, H. Ahlenius, C.J.H. Pronk, S. Bonde, Z. Kokaia, S.-E. W. Jacobsen, O. Lindvall, Tumor necrosis factor receptor 1 is a negative regulator of progenitor proliferation in adult hippocampal neurogenesis, J. Neurosci. 26 (2006) 9703–9712, https://doi.org/10.1523/JNEUROSCI.2723-06.2006.

[39] A.M. Jurga, M. Paleczna, K.Z. Kuter, Overview of general and discriminating markers of differential microglia phenotypes, Front. Cell. Neurosci. 14 (2020) 198, https://doi.org/10.3389/FNCEL.2020.00198.

[40] T. Miyashita, S. Kubik, G. Lewandowski, J.F. Guzowski, Networks of neurons, networks of genes: an integrated view of memory consolidation, Neurobiol. Learn. Mem. 89 (2008) 269–284, https://doi.org/10.1016/J.NLM.2007.08.012.

[41] K. Brami-Cherrier, E. Roze, J.-A. Girault, S. Betuing, J. Caboche, Role of the ERK/MSK1 signalling pathway in chromatin remodelling and brain responses to drugs of abuse, J. Neurochem. 108 (2009) 1323–1335, https://doi.org/10.1111/J.1471-4159.2009.05879.X.

[42] A.V. Tzingounis, R.A. Nicoll, Arc/Arg3.1: linking gene expression to synaptic plasticity and memory, Neuron 52 (2006) 403–407, https://doi.org/10.1016/J.NEURON.2006.10.016.

[43] M. Ghowsi, H. Khazali, S. Sisakhtnezhad, Evaluation of *TNF*-α and *IL-6* mRNAs expressions in visceral and subcutaneous adipose tissues of polycystic ovarian rats and effects of resveratrol, Iran, J. Basic Med. Sci. 21 (2018) 165–174, https://doi.org/10.22038/IJBMS.2017.24801.6167.

[44] K.J. Livak, T.D. Schmittgen, Analysis of relative gene expression data using real-time quantitative PCR and the $2^{-\Delta\Delta C}_{T}$ method, Methods 25 (2001) 402–408, https://doi.org/10.1006/METH.2001.1262.

[45] M. Bolós, J.R. Perea, J. Avila, Alzheimer's disease as an inflammatory disease, Biomol. Concepts 8 (2017) 37–43, https://doi.org/10.1515/BMC-2016-0029.

[46] Y. Tang, W. Le, Differential roles of M1 and M2 microglia in neurodegenerative diseases, Mol. Neurobiol. 53 (2016) 1181–1194, https://doi.org/10.1007/S12035-014-9070-5.

[47] X.Y. Xiong, L. Liu, Q.W. Yang, Functions and mechanisms of microglia/macrophages in neuroinflammation and neurogenesis after stroke, Prog.

Neurobiol. 142 (2016) 23–44, https://doi.org/10.1016/J.PNEUROBIO.2016.05.001.
[48] A. Dobolyi, C. Vincze, G. Pál, G. Lovas, The neuroprotective functions of transforming growth factor beta proteins, Int. J. Mol. Sci. 13 (2012) 8219–8258, https://doi.org/10.3390/IJMS13078219.
[49] E. Colombo, C. Farina, Astrocytes: key regulators of neuroinflammation, Trends Immunol. 37 (2016) 608–620, https://doi.org/10.1016/J.IT.2016.06.006.
[50] E. Tyagi, R. Agrawal, C. Nath, R. Shukla, Cholinergic protection via α7 nicotinic acetylcholine receptors and PI3K-Akt pathway in LPS-induced neuroinflammation, Neurochem. Int. 56 (2010) 135–142, https://doi.org/10.1016/J.NEUINT.2009.09.011.
[51] M. Yamamoto, T.W. Kensler, H. Motohashi, The KEAP1-NRF2 system: a thiol-based sensor-effector apparatus for maintaining redox, Homeostasis 98 (2018) 1169–1203, https://doi.org/10.1152/PHYSREV.00023.2017.
[52] R. Feng, Y. Morine, T. Ikemoto, S. Imura, S. Iwahashi, Y. Saito, M. Shimada, Nrf2 activation drive macrophages polarization and cancer cell epithelial-mesenchymal transition during interaction, Cell Commun. Signal. 16 (2018) 54, https://doi.org/10.1186/S12964-018-0262-X.
[53] R. Knoth, I. Singec, M. Ditter, G. Pantazis, P. Capetian, R.P. Meyer, V. Horvat, B. Volk, G. Kempermann, Murine features of neurogenesis in the human Hippocampus across the lifespan from 0 to 100 years, PLoS One 5 (2010), e8809, https://doi.org/10.1371/JOURNAL.PONE.0008809.
[54] M. Izvolskaia, V. Sharova, L. Zakharova, Prenatal programming of neuroendocrine system development by lipopolysaccharide: long-term effects, Int. J. Mol. Sci. 19 (2018) 3695, https://doi.org/10.3390/IJMS19113695.
[55] R. Beloosesky, Z. Weiner, N. Khativ, N. Maravi, R. Mandel, J. Boles, M.G. Ross, J. Itskovitz-Eldor, Prophylactic maternal n-acetylcysteine before lipopolysaccharide suppresses fetal inflammatory cytokine responses, Am. J. Obstet. Gynecol. 200 (2009), https://doi.org/10.1016/J.AJOG.2009.01.032, 665.e1–e5.
[56] J.S.C. Chua, C.J. Cowley, J. Manavis, A.M. Rofe, P. Coyle, Prenatal exposure to lipopolysaccharide results in neurodevelopmental damage that is ameliorated by zinc in mice, Brain Behav. Immun. 26 (2012) 326–336, https://doi.org/10.1016/J.BBI.2011.10.002.
[57] W.K. Nahm, J.L. Noebels, Nonobligate role of early or sustained expression of immediate-early gene proteins c-fos, c-jun, and zif/268 in hippocampal mossy fiber sprouting, J. Neurosci. 18 (1998) 9245–9255, https://doi.org/10.1523/JNEUROSCI.18-22-09245.1998.
[58] J.F. Guzowski, Insights into immediate-early gene function in hippocampal memory consolidation using antisense oligonucleotide and fluorescent imaging approaches, Hippocampus 12 (2002) 86–104, https://doi.org/10.1002/HIPO.10010.
[59] Y.-J. Gao, R.-R. Ji, c-Fos or pERK, which is a better marker for neuronal activation and central sensitization after noxious stimulation and tissue injury? Open Pain J. 2 (2009) 11–17, https://doi.org/10.2174/1876386300902010011.
[60] J.P.E. Spencer, Beyond antioxidants: the cellular and molecular interactions of flavonoids and how these underpin their actions on the brain, Proc. Nutr. Soc. 69 (2010) 244–260, https://doi.org/10.1017/S0029665110000054.
[61] R.J. Williams, J.P.E. Spencer, Flavonoids, cognition, and dementia: actions, mechanisms, and potential therapeutic utility for Alzheimer disease, Free Radic. Biol. Med. 52 (2012) 35–45, https://doi.org/10.1016/J.FREERADBIOMED.2011.09.010.
[62] K. Hoshino, K. Hasegawa, H. Kamiya, Y. Morimoto, Synapse-specific effects of IL-1β on long-term potentiation in the mouse hippocampus, Biomed. Res. 38 (2017) 183–188, https://doi.org/10.2220/BIOMEDRES.38.183.
[63] T. Takemiya, K. Fumizawa, K. Yamagata, Y. Iwakura, M. Kawakami, Brain interleukin-1 facilitates learning of a water maze spatial memory task in young mice, Front. Behav. Neurosci. 11 (2017) 202, https://doi.org/10.3389/FNBEH.2017.00202.
[64] Y. Tozuka, S. Fukuda, T. Namba, T. Seki, T. Hisatsune, GABAergic excitation promotes neuronal differentiation in adult hippocampal progenitor cells, Neuron 47 (2005) 803–815, https://doi.org/10.1016/J.NEURON.2005.08.023.
[65] L. Wang, A. Shiraki, M. Itahashi, H. Akane, H. Abe, K. Mitsumori, M. Shibutani, Aberration in epigenetic gene regulation in hippocampal neurogenesis by developmental exposure to manganese chloride in mice, Toxicol. Sci. 136 (2013) 154–165, https://doi.org/10.1093/TOXSCI/KFT183.
[66] H. Asada, Y. Kawamura, K. Maruyama, H. Kume, R.-G. Ding, N. Kanbara, H. Kuzume, M. Sanbo, T. Yagi, K. Obata, Cleft palate and decreased brain γ-aminobutyric acid in mice lacking the 67-kDa isoform of glutamic aciddecarboxylase, Proc .Natl .Acad .Sci .U .S.A 94 (1997) 6496–6499, doi.org/10.1073/PNAS.94.12.6496.
[67] F.C. Roth, A. Draguhn, GABA metabolism and transport: effects on synaptic efficacy, Neural Plast. (2012) 805830, https://doi.org/10.1155/2012/805830, 2012.
[68] S.C. Danzer, J.O. McNamara, Localization of brain-derived neurotrophic factor to distinct terminals of mossy fiber axons implies regulation of both excitation and feedforward inhibition of CA3 pyramidal cells, J. Neurosci. 24 (2004) 11346–11355, https://doi.org/10.1523/JNEUROSCI.3846-04.2004.
[69] P. Berghuis, M.B. Dobszay, K.M. Sousa, G. Schulte, P.P. Mager, W. Härtig, T. J. Görcs, Y. Zilberter, P. Ernfors, T. Harkany, Brain-derived neurotrophic factor controls functional differentiation and microcircuit formation of selectively isolated fast-spiking GABAergic interneurons, Eur. J. Neurosci. 20 (2004) 1290–1306, https://doi.org/10.1111/J.1460-9568.2004.03561.X.
[70] J. Boulanger-Bertolus, A.-M. Mouly, Ultrasonic vocalizations emission across development in rats: coordination with respiration and impact on brain neural dynamics, Brain Sci. 11 (2021) 616, https://doi.org/10.3390/BRAINSCI11050616.
[71] G. Blázquez, A. Castañé, A. Saavedra, M. Masana, J. Alberch, E. Pérez-Navarro, Social memory and social patterns alterations in the absence of STriatal-enriched protein tyrosine phosphatase, Front. Behav. Neurosci. 12 (2019) 317, https://doi.org/10.3389/FNBEH.2018.00317.
[72] K.A. Huckleberry, F. Shue, T. Copeland, R.A. Chitwood, W. Yin, M.R. Drew, Dorsal and ventral hippocampal adult-born neurons contribute to context fear memory, Neuropsychopharmacology 43 (2018) 2487–2496, https://doi.org/10.1038/s41386-018-0109-6.
[73] S. Maren, K.L. Phan, I. Liberzon, The contextual brain: implications for fear conditioning, extinction and psychopathology, Nat. Rev. Neurosci. 14 (2013) 417–428, https://doi.org/10.1038/nrn3492.